Optically Stimulated Luminescence Dating as a Geochronological Tool for Late Quaternary Sediments in the Red Sea Region

David C. W. Sanderson and Timothy C. Kinnaird

Abstract

This chapter concerns the use of luminescence methods as geochronological tools for dating Late Quaternary sediments in the Red Sea region. The dating methods all use stimulated luminescence to register signals developed in mineral systems in response to long term exposure to ionising radiation in the environment. The principles of luminescence dating are outlined followed by discussion of its application to the Arabian Peninsula, where, particularly in SE Arabia and parts of the interior, a growing corpus of work is emerging, which is helping to define past arid or humid periods of importance to palaeoclimatology and to archaeology. Turning to the Red Sea, studies conducted within the DISPERSE project are presented both in marine and terrestrial settings. The motivation for much of this work concerns definition of the environmental conditions and chronologies for hominin and human dispersion through Arabia. Data are presented which identify, for the first time, late Pleistocene evidence on the inner continental shelf near the Farasan Islands, using material from the 2013 cruise of RV AEGAEO. Results are also presented from the littoral fringe of southwest Saudi Arabia, identifying units associated with MIS5 which have palaeo-environmental and archaeological significance. It is to be hoped that further research in coming decades will continue to extend the regional chronology for the littoral fringe of the Red Sea. In this respect, luminescence dating has the potential to help define the environmental history of this important area, to assist with assigning marine and terrestrial features into unique stages of Quaternary climate cycles, and to promote better understanding of human-environment interactions in this dynamic area.

D. C. W. Sanderson (✉)
Scottish Universities Environmental Research Centre (SUERC), East Kilbride, UK
e-mail: david.sanderson@glasgow.ac.uk

T. C. Kinnaird
School of Earth and Environmental Sciences, University of St. Andrews, St Andrews, UK

T. C. Kinnaird
School of Biological and Environmental Sciences, University of Stirling, Stirling, UK

N. M. A. Rasul and I. C. F. Stewart (eds.), *Geological Setting, Palaeoenvironment and Archaeology of the Red Sea*,
https://doi.org/10.1007/978-3-319-99408-6_31

1 Introduction

Optically stimulated luminescence, and its related variants, have emerged in recent decades as important geochronometric tools for constraining sediment formation ages and post-depositional processes in many Quaternary palaeo-environments, including those of the Red Sea region. In this chapter, the underlying principles and age limits of luminescence dating are outlined. Examples are discussed of work which has defined the age limits of relic dune systems in the Arabian Peninsula, and studies conducted within the DISPERSE project on the littoral fringe of southwest Saudi Arabia and from marine cores off the coast of the Farasan Islands. The results confirm the utility of luminescence dating to palaeo-environmental work in the Red Sea region, and testify to varied environmental conditions in the past, which make this area critical for studies of human dispersal and occupation during Palaeolithic periods.

2 Luminescence Dating of Sediments

Luminescence dating is part of a class of radiation damage dating methods, which include electron spin resonance (ESR) dating and methods based on stimulated luminescence of minerals, by heat, as in thermoluminescence (TL), or light, as in photostimulated luminescence (PSL) or optically stimulated luminescence (OSL). In these methods, prolonged exposure to ionising radiation in the physical environment deposits energy, releasing electrons and holes from their normal bound states in insulating minerals. Charge-trapping at meta-stable defect centres within the

mineral lattice can store energy and, through evolution of populations of trapped charge carriers, can store quantum information concerning radiation exposure, optical exposure and thermal history. By stimulated release of trapped charge, using heat or light, and subsequent relaxation of the system, low level light emission occurs, which can be detected and quantified using photon counting methods.

The intensity of luminescence signals depends on the extent of prior exposure to natural radiation since an earlier zero condition, and on the sensitivity of the individual minerals, which has a complex dependence on formation and post formation conditions. In dating techniques, a series of calibration experiments are undertaken, with laboratory radiation sources, to quantify the natural luminescence signal in terms of "equivalent dose". This corresponds to the radiation dose (in units of Grays, which are a measure of energy deposition per unit mass) which would account for the natural signals observed from the mineral system under study. In parallel with the equivalent dose determination, a combination of low-level radiometric measurements, radionuclide concentration measurements, and dosimetric modelling is used to define palaeo-dose rates from the sample and its environment. The luminescence age is then determined as the quotient of equivalent dose to the estimated palaeo-dose rate.

Figure 1 provides a schematic illustration of the evolution of luminescence signals in a hypothetical mineral from geological formation, to deposition within a sediment, and final laboratory processing. Since primary mineral formation processes, whether from high or low temperature crystallization, should not introduce initial trapped charge populations to the structural defects, the initial post formation state corresponds with no potential for generating stimulated luminescence. The complex geological, thermal and radiation histories experienced by minerals which can include multiple cycles of diagenetic alteration, irradiation, thermal exposure, weathering and sedimentation over long periods, have the potential both to affect the defect configuration within mineral lattices, and their state of electronic and hole population. Early research exploring the potential for using TL to directly date the formation of geological materials (e.g., McDougall 1968) demonstrated that defect filling by ionising radiation (for example the alpha, beta and gamma radiation from the natural decay series, primordial nuclides and cosmic radiation) tends to proceed significantly faster than defect formation (for example by recoil damage during internal alpha decay or spontaneous fission, or by alterations). Therefore, geological-cycle luminescence is generally expected to saturate at levels whereby the thermal stabilities of trapped charge carriers are in a pseudo-equilibrium with their environmental conditions. This view has prevailed as a paradigm, which leads luminescence dating applications toward more recent periods whereby target dating events follow a "zeroing event", such as heating (in synthetic materials like ceramics, during firing, or in the case of heated lithics, by natural or artificial processes), or significant light exposure which "bleaches" the potential signals during terminal cycles of weathering and sedimentary deposition. It is of course easy to see that there are some geological history pathways which can lead to multiple cycles of signal evolution and diminution, as well as to changes in defect populations and configurations prior to such a "zeroing event". Some of these are illustrated schematically by the multiple pathways in the geological part of Fig. 1.

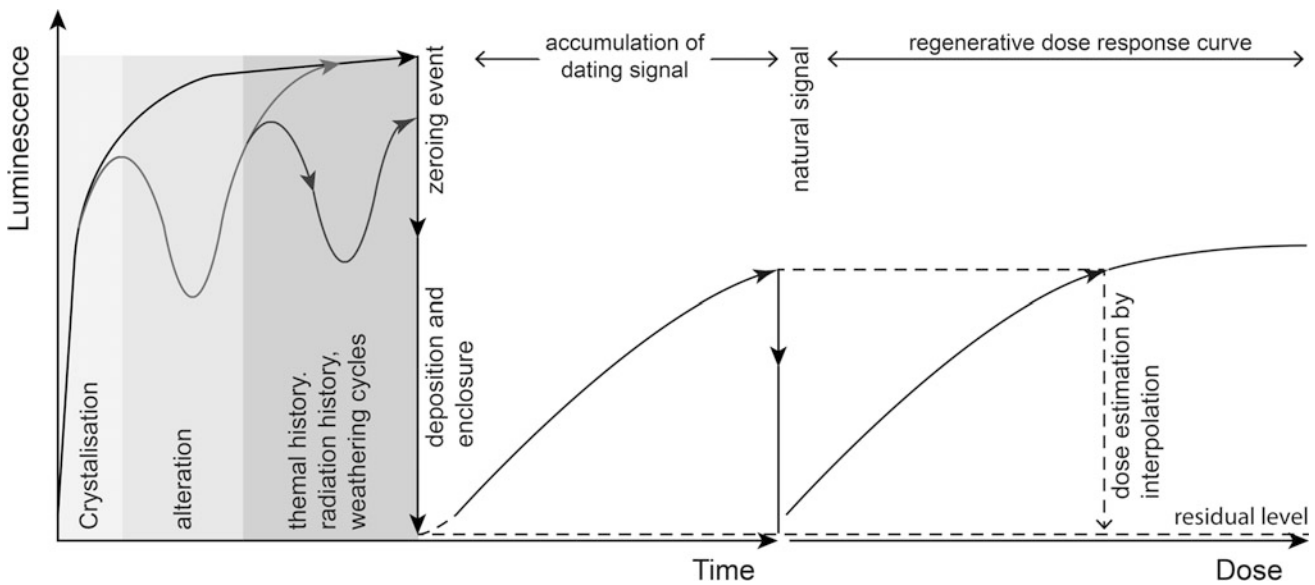

Fig. 1 Illustration of the luminescence signal evolution in a hypothetical mineral during its geological history, the period of natural accumulation following sedimentary deposition, and during laboratory measurement cycles

Zeroing by optical exposure can be envisaged as a consequence of energy capture of photons by trapped electron or hole populations, resulting in promotion from localized states in point defects to conduction and valance bands, from where charge transport and eventual relaxation can take place. The optical transitions associated with de-trapping can be direct or indirect, whereby photon and thermal energies are both involved. The relaxation processes are potentially complex since optical bleaching at environmental temperatures can also be associated with re-trapping. Nevertheless, the end result of bleaching is to reduce the latent luminescence signals to residual levels, close to zero. Enclosure following sedimentary deposition and protection from further light exposure leads to a new period of natural accumulation, in response to further exposure to ionising radiation in the environment. Thus, the potential luminescence signal increases again, during the accumulation period. The aim of luminescence dating, as indicated above, and in general accounts of the method (e.g., Aitken 1985, 1998), is to measure and quantify the radiation dose equivalent to the accumulation of the dating signal, and to assess the elapsed time by comparison with the integrated environmental dose rate required to generate the equivalent dose.

Figure 1 also illustrates the signal trajectory following sampling, and mineral separation in the laboratory, both of which are conducted under subdued lighting conditions, and during dose quantification. Measurement of the natural luminescence signal by stimulation in the laboratory once again depletes the signal. Quantification using regenerative methods involves the use of calibrated radiation sources to develop dose response curves, which can be interpolated to determine the equivalent dose. This approach is illustrated schematically in Fig. 1. Another approach that could be considered would be to prepare multiple portions of the samples and apply the method of standard additions, as illustrated in Fig. 2, to estimate equivalent doses, in which case an appropriate dose response function must be fitted to the data set and extrapolated. This method can also be combined with regenerative approaches.

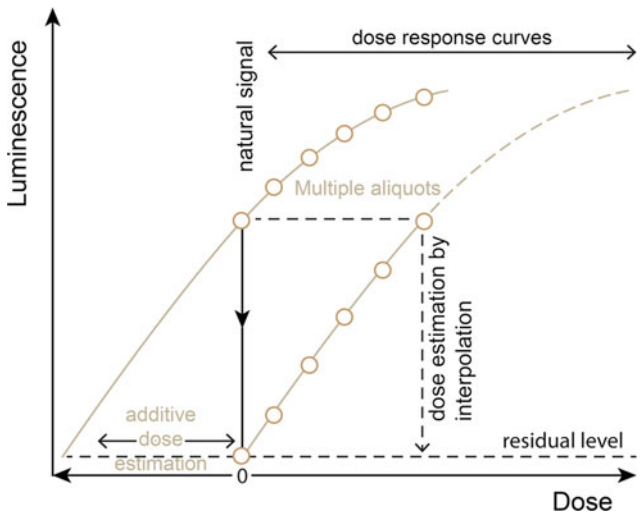

Fig. 2 Illustration of the additive dose estimation approach, and combined additive-regenerative approaches

With these considerations in mind, for sediments which have (i) been effectively zeroed prior to last deposition (for example by light exposure, or by heat), (ii) which have not been subject to post-depositional alterations, (iii) whose luminescence signals are retained with stability, and (iv) whose dose response characteristics can be reconstructed in the laboratory without bias, luminescence ages correspond to the physical time interval since deposition. For systems with more complex behaviour or origins, the system can deliver information on depositional and post-depositional conditions which may be of value in combination with other information to help constrain understanding of sedimentary records. The system is also capable of yielding information about past thermal histories, and of registering the effects of prolonged light exposure to lithic surfaces.

While the luminescence phenomena used for TL, OSL and related dating systems can be observed from most translucent minerals, the majority of geochronometric studies have been applied to quartz or feldspar systems. Age limits depend on defect configuration and luminescence properties of individual quartzes and feldspars. Luminescence sensitivity and the completeness of pre-depositional zeroing set the lower age limit, which can be less than a few years for the feldspar system, and below 100 years for sufficiently bright quartz. Upper age limits are set by a combination of signal stability and by the saturation limits associated with finite defect populations within target minerals.

For quartz OSL dating, the upper limit of saturation is usually found in the 100–200 Gy dose range, corresponding to ages of approximately 2×10^5 years depending on dose rates. As the system approaches saturation, there is some degradation of precision and resolution, typically observed above approximately 100 ka. Notwithstanding this, the quartz OSL dating system is well established now within the 10^2–10^5 year age range as a geochronometer with increasing applications. There are also deep trap signals from quartz with potential for age extension, up to 10^6 years, on a research basis, of which phototransferred thermoluminescence (PTTL) (Sanderson et al. 2001), thermally transferred OSL (TT-OSL) (Wang et al. 2006; Adamiec et al. 2008, 2010), and high temperature phosphorescence (Kinnaird et al. 2010) are perhaps the more promising approaches. Quartz OSL ages are mostly measured using regenerative dose response techniques, such as the single-aliquot regenerative (SAR) method. Here many aliquots, or even single

quartz grains are studied, and dose distributional analysis used as a means of identifying mixed-age, or incompletely bleached samples.

The feldspar systems have greater sensitivity and uniformity than quartz-based systems, but are associated with an unenviable reputation for instability, which must be examined explicitly within dating procedures. Feldspar luminescence can be stimulated in many wavebands from UV to near IR, and is associated with complex distributions of trapping systems with a wide variety of kinetic behaviour. Dose response curves continue to grow into the 1–10 kGy region, which corresponds to age limits of approximately 1 Ma, providing stability can be assured. Thermally stabilized single aliquot regenerative-additive dose (SARA) procedures (Kinnaird et al. 2015a), the use of high temperature post-IR infrared stimulated luminescence (pIR-IRSL) (Thomsen et al. 2008; Buylaert et al. 2009), and the use of near UV stimulation bands are some of the approaches under consideration for applying feldspar based luminescence methods to early Quaternary systems.

Effective sampling is of critical importance to successful sediment dating, and there has been significant recent progress in the development of simple luminescence profiling methods (Sanderson and Murphy 2010), which can be applied both in the field, using portable luminescence readers, and in the laboratory, to characterise complex sediment sequences, and identify discontinuities (e.g., the Pleistocene/Holocene discontinuity illustrated below in core FA13), inversions and potentially mixed units. When used in combination with quantitative laboratory dating procedures these approaches seem to be useful for defining the context of dating materials.

3 An Overview of Luminescence Dating Studies in the Red Sea Region and Arabian Peninsula

Given the spatial scale of the Arabian Peninsula (about 3.24 million km^2) and the Red Sea (which encloses an area of 0.438 million km^2, with a linear coastal dimension of some 2250 km) there are, so far, comparatively few luminescence dates from the coastal region. However, the opportunities can readily be perceived, given the nature of land cover and the relatively recent, on a geological timescale, rifting which formed the Red Sea.

One strand of enquiry concerns aridity history. Luminescence dating has been associated with drylands research since the inception of the first thermoluminescence dates for sediments in the late 1970's. Following the initial demonstration that marine cores showed a stratigraphic progression of thermoluminescence ages, and the recognition of the role of optical bleaching in resetting the system (Wintle and Huntley 1979), Singhvi et al. (1982, 1983) reported dating of sand dunes in drylands in Rajastan. The TL methods used at that time had residual signals, and early work explored means of estimating their magnitude. The development of optical stimulation approaches, initially using filtered green lasers (Huntley et al. 1985), and later with diverse stimulation sources (Bøtter-Jensen et al. 2000) has greatly facilitated the analysis of sediments.

In respect of drylands research on the Arabian Peninsula, McClure (1976) identified phases of lake development in the Mundafan basin (Rub al Khali) between 36–21 ka and 9–6 ka (uncalibrated radiocarbon years), indirectly constraining the associated dune formations to the intervening and succeeding arid periods. Glennie and Singhvi (2002) have outlined interactions between glacially forced sea level in the Arabian Gulf, exposing the floor during low-stands, and the palaeoclimatic systems. Given the modern interplay between dry "Shamal" winds from the north, and the moist NE and SW monsoon cycles, an analogous framework was proposed for earlier cycles to account for the transfer of carbonate rich sediments to SE Arabia, during dry cold periods of the Quaternary, and subsequent alteration and redistribution in more humid periods. Issues concerning radiocarbon dating, particularly of carbonate fractions, were discussed and some 30 luminescence dates from dunes sands were presented. When classified by sedimentary setting into Shamal, and Monsoon linked categories, associations between the generalised sea-level curve of Boulton (1993) and the ages of the two types of sediments were notable. These data broadly supported the framework outlined above, linking arid periods to the glacial cycle. On this basis arid conditions have been experienced back to some 350 ka with more humid periods, during the interstadials, when weaker Shamal winds and a stronger SW Monsoon may have been experienced. This framework has been extended further in SE Arabia. Bray and Stokes (2003, 2004) examined a one metre core from Liwa in the UAE, producing 12 OSL dates of which the upper 55 cm ranged from 2.5–3.2 ka, grading upward to 6–7 ka at the base of the core. They suggested that the transition between humid early Holocene conditions (about 10 ka–6 ka) and the arid conditions which followed was accompanied by a local lag time, as older dune sands in the Rub al Khali were reworked. Speleothem records from northern Oman (Burns et al. 1998) provide another record which is broadly consistent with this framework. Preusser et al. (2002) discussed a suite of 74 IRSL dates obtained from cores in the Wahiba sands in Oman, which ranged from MIS1 back to MIS6. From these data, periods of sand movement were inferred in MIS1, the earlier part of MIS2, MIS4 leading into MIS5a, MIS5d leading into 5e, and MIS6.

Additional studies in SE Arabia include the UAE (Glennie et al. 2011; Farrant et al. 2015; Preston et al. 2015), Oman (Blechschmidt et al. 2009; Preusser et al. 2002;

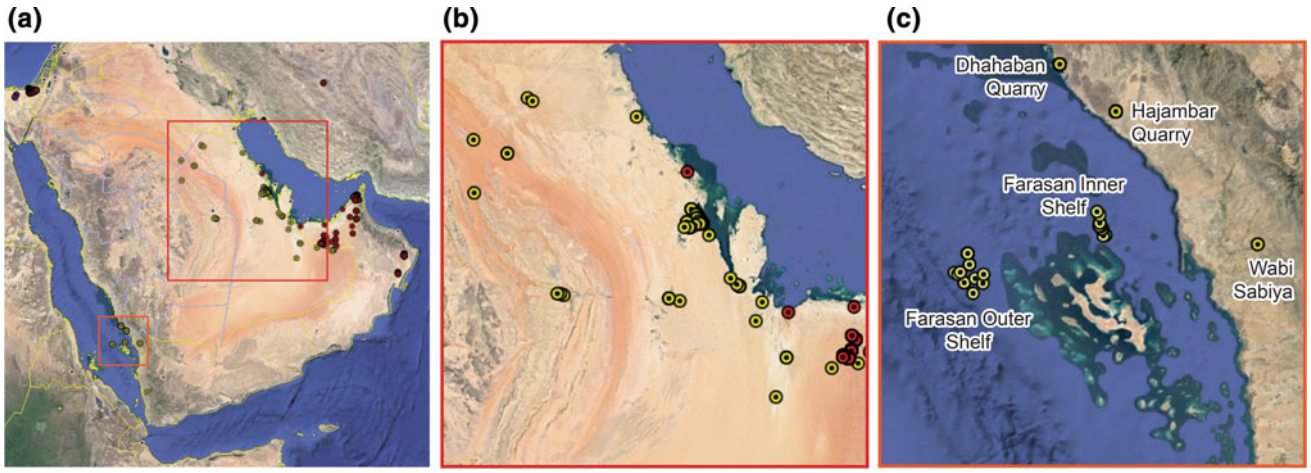

Fig. 3 Location map showing the distribution of luminescence dating samples referred to in the text. Red symbols (left and middle maps) are from the INQUA dune atlas database. Yellow symbols are from SUERC data, combining Saudi Aramco commissioned work in eastern Saudi Arabia, and Munro's samples in Yemen (left and middle maps) with samples from the recent DISPERSE project (right map)

Preusser 2009; McClaren et al. 2009; Matter et al. 2015; Hilbert et al. 2015; Hoffman et al. 2015), and parts of Yemen and Saudi Arabia (Munro and Wilkinson 2007; Munro et al. 2013). Duller (2016) reviewed some 385 luminescence dates from Arabia, associated with the INQUA dune Atlas (Lancaster et al. 2016), the majority of which are from the UAE or Oman (Fig. 3a). He draws attention to the different luminescence dating approaches used in these studies, noting that within the current uncertainties on luminescence dating the task of disentangling individual MIS stages remains challenging. While the majority of determinations reviewed fall in the last 100 ka, some 31% are older, which include IRSL feldspar data, where stability limits may be in question, and quartz OSL data where signal saturation may be a limiting factor. The emergence of age extension methods, such as TT-OSL, pIR-IRSL, and other techniques with potential to respond to stable deep-trap signals with high saturation dose responses, and related techniques are clearly important to extending luminescence chronologies to the early Quaternary.

While Munro's earlier investigations (Munro and Wilkinson 2007) also were concerned with aridity/humidity cycles in Yemen and Saudi Arabia, his later summary (Munro et al. 2013) also had access to more than 70 additional OSL dates from Late Quaternary sediments in Saudi Arabia commissioned by Stephen Franks on behalf of Saudi Aramco and conducted at SUERC (Burbidge et al. 2007a; Cresswell and Sanderson 2009). These were collected (Fig. 3b) with the primary aim of assessing the conditions and durations of formation of clay coatings on quartz sands during cyclic aridity phases, as a means of validating porosity models applied to resource reservoirs. However, the data from these studies, which included a series of samples covering wadi and sabkha systems, also placed constraints on the aridity history of the recent environment, confirming that cemented and altered palaeo-dune surfaces imply a diverse range of environmental and climatic conditions in the past, including humid and arid cycles that reach back to before 275 ka. It was noted in this work that uranium anomalies, with atypical U/Th ratios were observed in some cases, in association with cemented sands. Since cementation itself is the product of at least one cycle of hydration and aridity and can, under some circumstances, re-deposit uranium and radium in series-disequilibrium, it is important that dose rate determination methods with the potential to detect such behaviour are used for such material.

A second strand of enquiry, where the coupling between Quaternary climatic cycles and the environment is critical, concerns hominin and human dispersal from Africa and particularly the southern migration routes to India, SE Asia and beyond. Whether a northern corridor from Africa through the Levant, or a southern crossing of the Red Sea are considered, the Arabian Peninsula presents both topographic and aridity barriers which are sensitive to timing. Dispersal may have been initiated in MIS5 or earlier, with potential routes through the interior of Arabia critically affected by climate, hydrology and seasonality. Potential southern migration routes along coastal fringes, and the possibility of southern crossings of the Red Sea, are also dependent on the effect on coastal regions of changing sea levels during glacial cycles. Petit-Maire et al. (2010) have presented U/Th dates for a palaeolake in Jordan which shows clear evidence of shells from MIS5 and earlier. Recent work conducted in currently arid parts of Arabia (Dennell and Petraglia 2012; Breeze et al. 2015; Groucott et al. 2015a, b, c; Jennings et al. 2015a, b; Parton et al. 2015a, b; Petraglia 2011; Petraglia et al. 2011, 2015; Scerri et al. 2015; Stimpson et al. 2015) has broadened the range of recognized environments in the

interior. Further south, others (Preusser 2009; Armitage et al. 2011; Rosenberg et al. 2011) have suggested that palaeo-environments associated with early anatomically-modern human (AMH) activity were present in Oman and the UAE at MIS5e. The role of movements of the inter-tropical convergence zone (ITCZ) in influencing palaeo-climates in Arabia has been noted by these authors. It remains an important research objective to link comprehensive and accurate chronologies for the aridity history of the region to the archaeological and faunal records and to the glacial cycle since access involving potential crossings of the southern Red Sea area and the Gulf would have been facilitated by low global sea levels, for example in MIS6, or in the later stages of MIS 5 or MIS4. From the above it will be seen that a great deal of information has been accumulated in recent years to confirm that current aridity of the region is not representative of the Quaternary past, and that humid periods have occurred, in the early Holocene and at several stages of the Pleistocene where conditions for human occupation and migration were favourable. While the direct chronological evidence linking climates and palaeo-environments still lacks the precision and detail needed, for high resolution modelling reconstruction, larger numbers of luminescence dates from sediments together with radiocarbon dating of the more recent materials, and U/Th dating of speleothems and other carbonates, are now available from Arabian contexts, particularly in the SE.

Turning to the Red Sea there is at present a far smaller body of luminescence dates, and a need for systematic work on the sediments of both the terrestrial margins and marine shelves of the littoral fringe in order to enhance understanding of the interplay between tectonics, climate, sea level and landscapes. Lambeck et al. (2011) have reviewed data and models for shoreline reconstruction in the recent Quaternary, taking account of isostatic and tectonic considerations as well as the available stratigraphies and surviving evidence of former coastlines with temporal constraints. It is clear that a more comprehensive set of chronological constraints is needed. In considering southern corridors for past crossing of the Red Sea during glacial low stands, it is significant to note that the Bab al Mandab is considered to have maintained a connection to the Indian Ocean at all stages, but that current models point to periods where short sea crossings may have been episodically available at times of minimum sea level (e.g., for short periods at 55 ka, 75 ka, and 100 ka; also within the time intervals 12–32 ka, 61–68 ka, and 94–96 ka). Bailey and coauthors (Bailey et al. 2007; Bailey and Flemming 2008; Bailey and King 2011) have made the case for systematic exploration of both marine and contiguous terrestrial areas in order to identify sites associated with Palaeolithic human activities and dispersion. The recent DISPERSE project has explored both parts of this on the Arabian side of the Red Sea (Bailey et al. 2015; Hausmann and Meredith-Williams 2016; Winder et al. 2015; Sakellariou et al., this volume). As part of this work, a series of luminescence profiling and dating analyses have been conducted at SUERC, from marine cores in the vicinity of the Farasan Islands, and from three terrestrial sites shown on the right-hand map of Fig. 3c.

4 Luminescence Dating and DISPERSE

The focus of DISPERSE research is on the western Arabian escarpment and the now-submerged territory of the southern Red Sea and has included field surveys on land and underwater and marine surveys offshore in the Farasan Islands. It also draws on comparative research in adjacent regions in the Near East and southern Levant. The work reported here focuses on two strands of this research: Firstly, the ongoing search for submerged, surviving fragments of Late Pleistocene landscapes (Sakellariou et al., this volume), with archaeological potential, on the Saudi Arabian continental shelf and secondly, archaeological and palaeo-geographical investigations on terrestrial coastal environments in SW Arabia (Sinclair et al., this volume; Inglis et al. 2014a). The following sections summarise the luminescence dating work conducted so far in support of these activities. Technical reports have further details (Kinnaird et al. 2015b, c).

5 Dating Sediment Cores from the Farasan Continental Shelf

As part of the search for surviving fragments of past littoral landscapes that formed during Pleistocene periods of lowered sea-level, a marine survey was conducted using the Hellenic Centre for Marine Research (HCMR) vessel AEGAEO in the Farasan region in May-June 2013. Multiple geophysical techniques were used to characterise the bathymetry of the sea-floor and the nature of the sub-surface (Sakellariou et al., this volume), and gravity cores were collected for later analysis. The aim of this study was to assess the potential of luminescence methods to classify the stratigraphy within such cores to date key samples from the material, to define sedimentation rates, and if possible to identify Pleistocene units. This survey targeted two regions on the outer and inner Farasan shelves respectively, as shown in Fig. 3c. These areas are characterised by different bathymetry; (i) the outer shelf has prominent terraces at 70–80 m depth and 38–40 m depth on the continental shelf, and 120 m depth on the continental slope, whereas (ii) the inner shelf comprises a 120 m deep elongate basin bounded by NW-SE normal faults, with bathymetric terraces at 70–75 m and 122 m depth. Eighteen gravity cores and 2 box cores were recovered to variable depths up to 4.5 m. Of these

cores, 10 cores were collected on the outer shelf, and 8 cores were collected on the inner shelf (Fig. 3c).

Sakellariou et al. (2013) summarized the cruise, locating samples and making initial interpretations of the geophysical and sedimentological data available from the gravity cores prior to further laboratory investigations. A subset of the cores was retained un-opened, to avoid potential light exposure, in order to facilitate luminescence profiling and dating.

6 Core Samples and Initial Luminescence Profiles

The available geophysical and sedimentological data for all the cores was reviewed, and on this basis, two cores were selected for initial luminescence investigation. Core FA6 (2.90 m long) was gathered (on 4/6/2013 at 17°02.35'N, 41° 11.23'E, at 83 m depth) from the outer shelf and core FA13 from the inner shelf (on 6/5/2013 at 17°12.838'N, 41° 55.131'E at a depth of 102 m). Both cores show magnetic susceptibility anomalies (Sakellariou et al. 2013); in FA6 at 205 cm depth (with Susceptibility Indices (SI) of 0 to 6–7), and in FA13 at 145 cm depth (from SI 0 to 3–4). A preliminary interpretation of the magnetic data was to raise the conjecture that it may be associated with the boundary between marine and terrestrial sediments (thus the Holocene and Late Pleistocene boundaries) (Sakellariou et al., this volume). Following the selection of the cores for luminescence characterisation and dating, the two cores were split under subdued light conditions at the HCMR and subsampled for screening using an SUERC portable OSL reader (Fig. 4). Sediment was extracted at regular intervals through both cores (about 10 cm), with tighter resolution sampling at the prominent breaks in the geophysical data, including the shift in magnetic susceptibility at 205 cm depth in FA6 and 145 cm in FA13. While the luminescence screening was being conducted under low light conditions as before, the other halves of the split cores were photographed and used to log the sedimentary sequences for the first time.

Luminescence profiles for IRSL, OSL, the IRSL/OSL ratio, and respective depletion indices were established using the methods described in Sanderson and Murphy (2010). These in turn were used to define a series of 'units' representing different episodes in the sedimentary and luminescence records, characterised by different trends and progressions in luminescence intensities with depth. This, in combination with the interpretation of the geophysical data, was used to select samples for further laboratory characterisation and quantitative luminescence dating. Material from the most promising zones for dating was identified, for example, where the initial profiles showed smooth downward progressions in luminescence signals. In addition, samples were taken for dating at prominent lithological breaks, and from above and beneath the magnetic susceptibility change.

Both cores showed increasing signal levels with depth. For core FA6 both IRSL and OSL showed similar depth progressions, spanning a dynamic range of one order of magnitude. Figure 5 shows the OSL profile alongside the original geophysical records. The changing OSL signal gradients around 150 cm may imply changing sedimentation rates, or changes in luminescence sensitivity gradients. To further assess these, and to gain an insight into the apparent age range implied by these signals, it is necessary to calibrate the material. This can be done either using an external radiation source on the bulk profiling samples or in the laboratory using prepared material (cf. Burbidge et al. 2007b). The pronounced magnetic susceptibility anomaly at 205 cm depth did not correspond with a step change in luminescence intensity, nor did the accompanying sedimentary logs show a fabric change, suggesting revision of the initial interpretation prior to opening the core.

The situation with core FA13 from the inner shelf is, however, different as shown in Fig. 6. Here OSL intensities

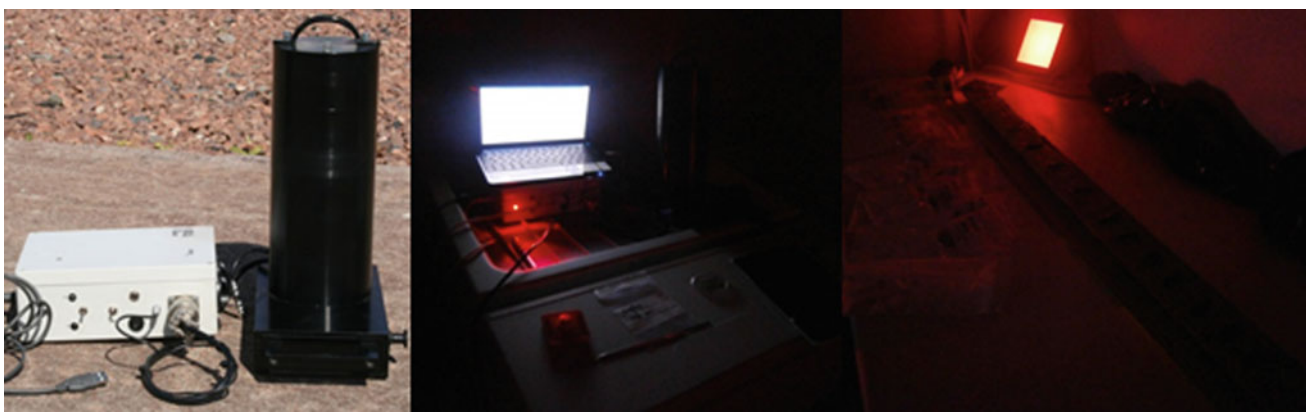

Fig. 4 Luminescence screening of cores FA6 and FA13 at HCMR using the SUERC portable OSL system (Sanderson and Murphy 2010)

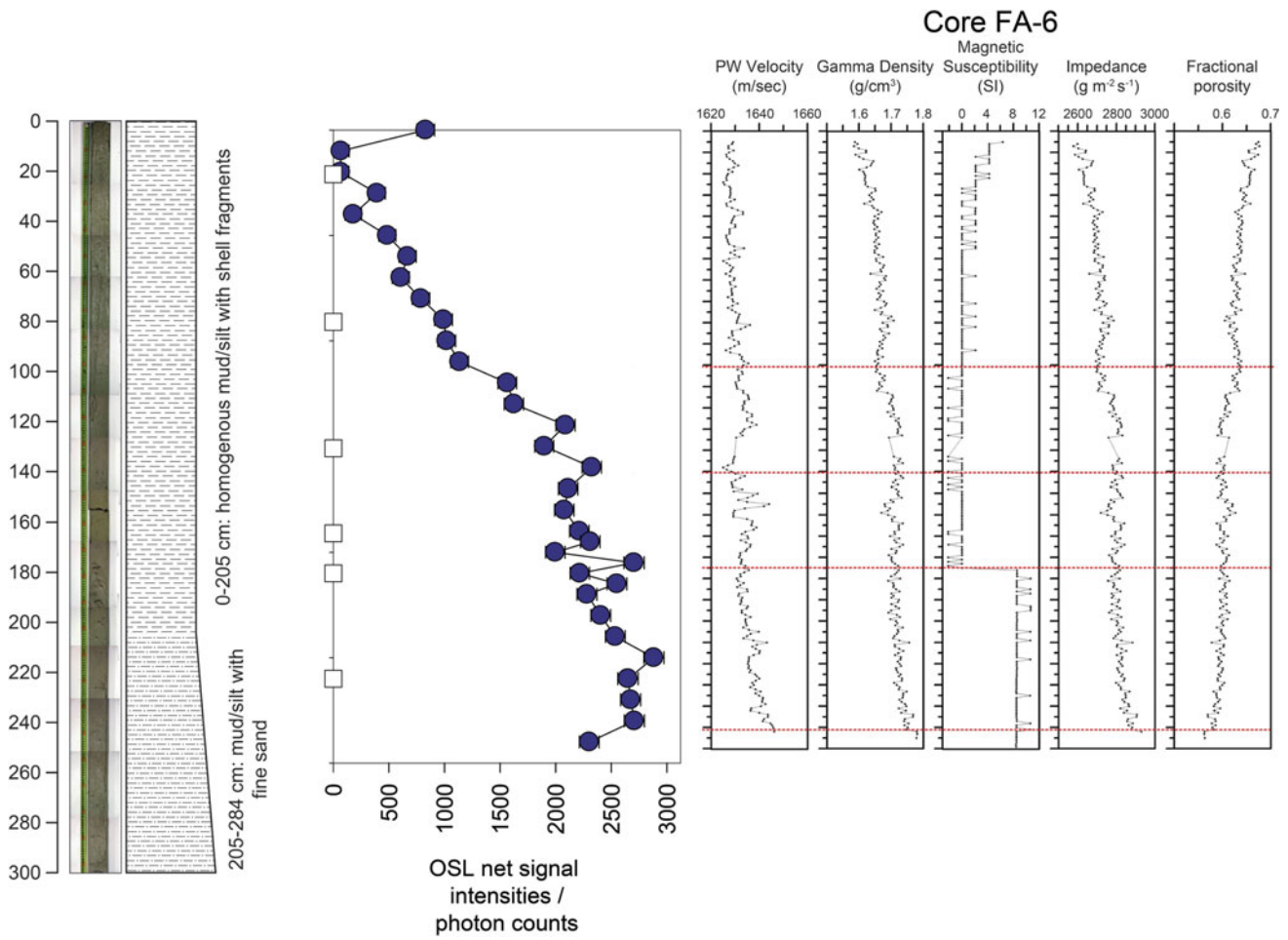

Fig. 5 OSL profile for core FA6 from the outer shelf, together with geophysical data

vary over 3 orders of magnitude, with similar signal levels to those observed in core FA6 for the upper 145 cm but with abrupt increases in signal intensities below this transition. This is accompanied by changes in sedimentary character and a series of magnetic susceptibility anomalies. At this stage of the analysis the evidence pointed toward the basal section of core FA13 as potentially exhibiting an age step corresponding to the Holocene/Pleistocene boundary, with FA6 most probably coming from younger material deposited at higher sedimentation rates in the outer shelf. The laboratory characterization and dating stages therefore aimed to assess these observations and interpretations.

7 Laboratory Profiling Measurements from Cores FA6 and FA13

Having thus established a relative framework, laboratory analysis progressed, first to calibrated luminescence screening and characterization of the profiling samples, then to quantitative dating runs from the samples selected above. Paired aliquots of 150–250 μm "quartz" and "polymineral" concentrates, and polymineral fines (4–11 μm) were prepared (cf., Burbidge et al. 2007b) and subjected to a simplified dose determination using a Risø DA15 OSL/TL reader. The reader was fitted with a combination of Schott BG39 + Corning 7/59 + Schott GG400 filters to detect in the region 390–450 nm, and isolate the main emission of the feldspar fraction. Although it might have been hoped that long range aeolian sands, potentially transported from Saharan or Arabian sources in different palaeoclimatic systems might have been present in the cores, quartz yields in 90–250 μm fractions were extremely low, particularly from the finer sediments in the upper parts of the cores. The quartz fractions recovered also exhibited low OSL sensitivities. Similarly, sand sized feldspar yields were limited with the exception of the coarser units at the base of core FA13. At this stage, it is unclear whether the absence of fine sands in the upper layers of the samples relates to the hydrodynamic processes associated with deposition and reworking of the marine sediments, or the limited quantities of Aeolian quartz being deposited at critical times in the development of the

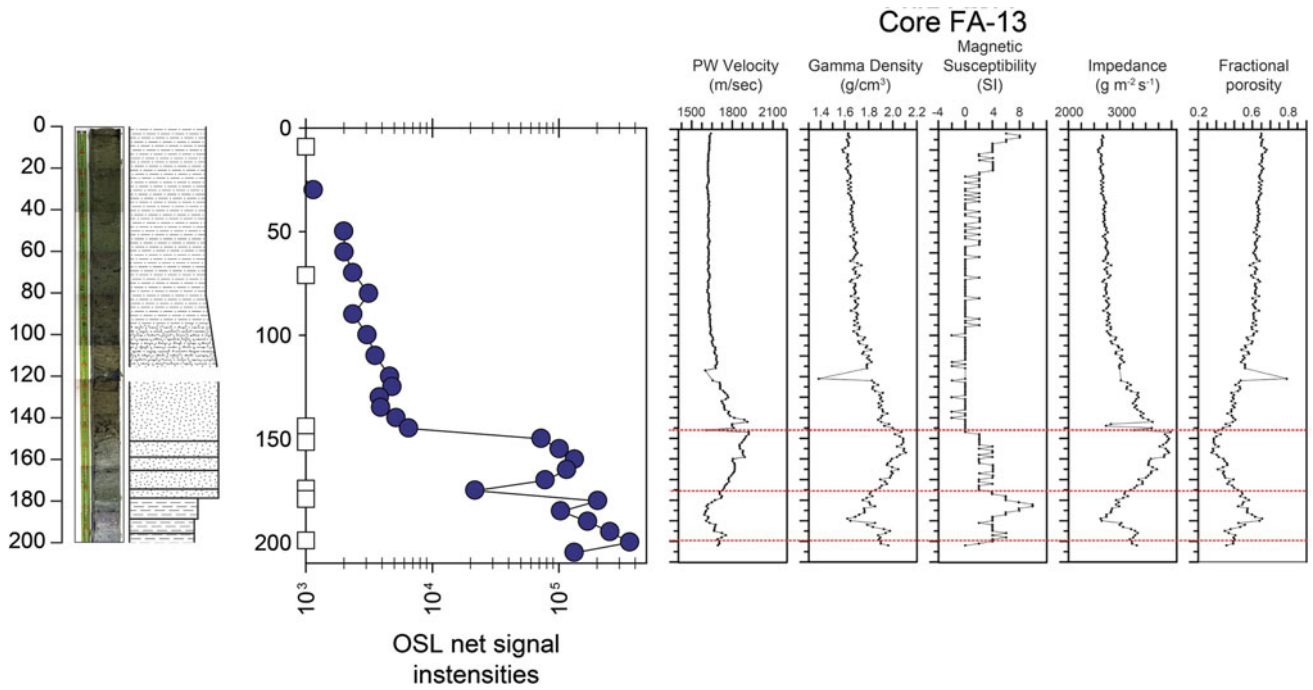

Fig. 6 OSL profiles from core FA13 from the inner shelf, together with geophysical data

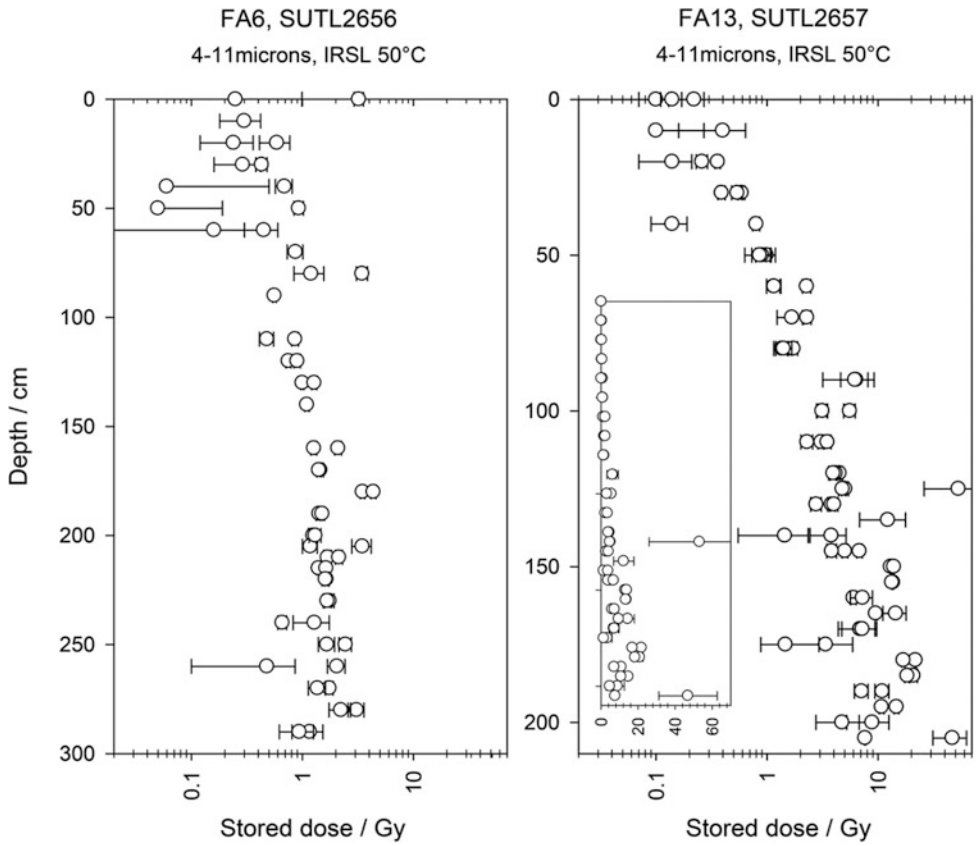

Fig. 7 Laboratory profiles from cores FA6 and FA13 showing the sedimentary logs, range of screening signals and stored dose values from each core

Table 1 Luminescence ages for cores FA6 and FA13

Core	SUTL no.	Depth (cm)	Total dose rate (mGy a^{-1})	IRSL SARA stored dose (Gy)	IRSL SAR stored dose (Gy)	Age (ka)
FA6	2658	20	0.38 ± 0.05	0.51 ± 0.03	–	1.4 ± 0.2
	2659	90	0.34 ± 0.04	–	0.36 ± 0.23	1.1 ± 0.7*
	2660	150	0.48 ± 0.09	–	0.63 ± 0.09	1.3 ± 0.3*
	2661	190	0.53 ± 0.06	2.05 ± 0.06	0.82 ± 0.13	1.6 ± 0.3*
	2662	210	0.51 ± 0.06	0.76 ± 0.20	–	1.5 ± 0.4
	2663	260	0.49 ± 0.06	2.85 ± 1.16	–	5.9 ± 2.5
FA13	2664	10	0.47 ± 0.05	0.95 ± 0.04	0.88 ± 0.22	2.1 ± 0.2
	2665	70	0.49 ± 0.05	2.73 ± 0.09	1.06 ± 0.19	5.6 ± 0.7
	2666	145	0.51 ± 0.05	0.51 ± 0.14	–	1.0 ± 0.3
	2667	150	0.68 ± 0.06	10.1 ± 0.55	19.9 ± 0.7	15.0 ± 1.5
	2668	175	0.64 ± 0.06	14.1 ± 1.5	13.5 ± 0.4	21.9 ± 3.2
	2669	180	1.70 ± 0.11	28.9 ± 9.0	24.2 ± 0.8	17.0 ± 5.4
	2670	200	1.10 ± 0.08	20.1 ± 4.4	25.2 ± 0.6	18.3 ± 4.2

cored sequences. However, fine grained (4–11 μm) polymineral fractions with good infra-red stimulated luminescence (IRSL) sensitivities were available from all samples producing depth-progressive stored dose estimates. This phase was therefore selected for dating both cores. Figure 7 shows the resulting dose profiles from both cores, reproducing the trends and maxima in the luminescence screening data. The stored dose values through the entirety of core FA6 and the upper part of FA13 were low, suggesting that these layers were likely to give later Holocene dates. Larger stored dose estimates, which in a low dose rate environment would correspond with substantially older dates, potentially of Late Pleistocene age, were only found at depth in core FA13.

Following the investigations outlined above, it was decided to exploit the fine (4–11 μm) polymineral phase in dating. Initially, equivalent dose determinations were made on 8 aliquots per sample using an IRSL SAR procedure (cf., Wallinga et al. 2000), with the objective of establishing whether reproducible data could be obtained, and to develop a dose response for the regenerative cycles (Table 1). Thereafter, dose estimates were obtained using an adapted SARA protocol, which incorporated long overnight preheats before first measurement to mitigate short-term fading effects (cf., Kinnaird et al. 2015a). The results of fading tests conducted between 6×10^5 s and 7×10^7 s indicate mean fading rates of 1.7 ± 0.014% per decade of time, suggesting that this worked. No further corrections for fading have therefore been made in the data which follow. In the original SARA method, groups of aliquots were formed with added doses, and a linear dose estimate made for each aliquot by scaling luminescence signals between the first (natural plus added dose) and a regenerated signal. Dose estimates are formed by regression of the added dose response curves to zero signal. In the modification suggested by Alexander (2007), long overnight preheating was introduced before the first readout, so that both natural and added doses are stabilised in the manner suggested by Sanderson (1988a). Automated readout with regenerative dose pre-heated in the instrument completes the sequence. This was implemented here with sets of 8 aliquots, sub-divided into 4 groups of 2 aliquots (natural, natural + β1, natural + β2, natural + β3). Irradiations were performed using an automated ELSEC irradiator equipped with a 1.85 GBq ^{90}Sr source (dose rate 1.76 Gy/min at the time of the experiment). The experimental conditions were as follows: IRSL from the natural and natural + β irradiated aliquots was recorded in a Risø DA15 reader, following 16 h preheating at 120°C. The samples were then irradiated within the reader, and their test dose responses were recorded after 30 s preheating at 220°C within the instrument. All IRSL measurements were conducted at 50°C for 60 s, with background signals recorded before and after stimulation. The data were reduced by integration and late light subtraction, and normalized IRSL

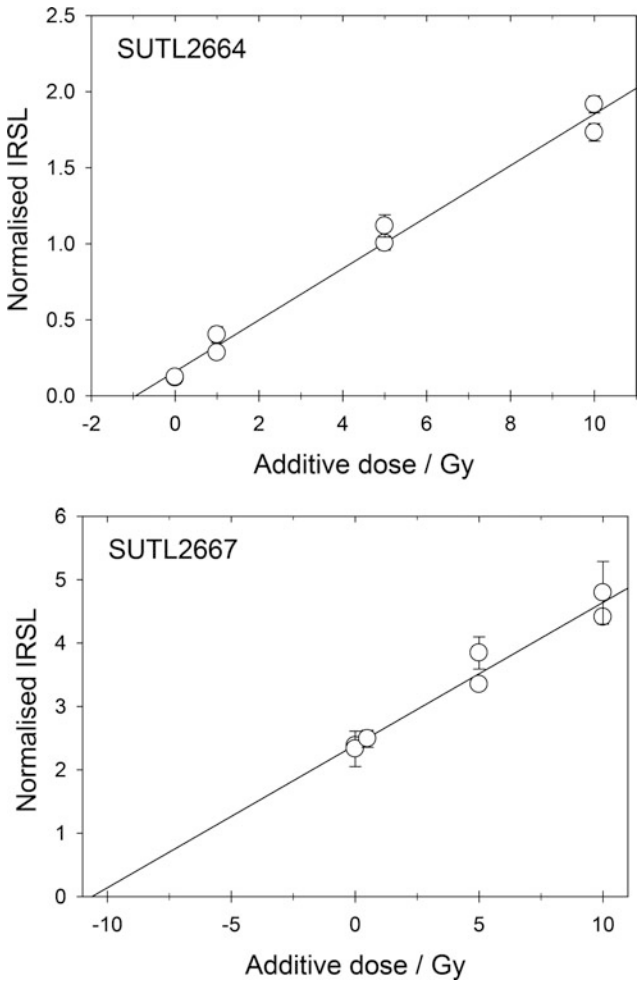

Fig. 8 IRSL SARA additive plots for the uppermost sample in FA13 (SUTL2664) and the first of the coarser units toward the base of the core (SUL2667)

ratios were used to construct additive dose response curves which were fitted by linear regression and extrapolated (using the methods of Scott and Sanderson 1988) to determine the stored doses. Figure 8 illustrates the process.

Dose rates to the dating materials were evaluated using analyses of the uranium, thorium and potassium concentrations obtained by HRGS coupled with beta dose rate measurement using TSBC (Sanderson et al. 1988b). As the sample quantity was limited, TSBC and HRGS measurements were performed on the same 20 g sub-sample, protected from light, and later used for mineral separations. To accommodate the low dose rates of these materials, duplicate 80 ks HRGS measurements were made. HRGS data, converted to dry infinite-matrix dose rates, were combined with beta dose rates, estimated water contents and alpha efficiency as inputs for the effective dose rate estimates. The contributions from the cosmic dose were modeled (Prescott and Stephan 1982; Prescott and Hutton 1988) by combining

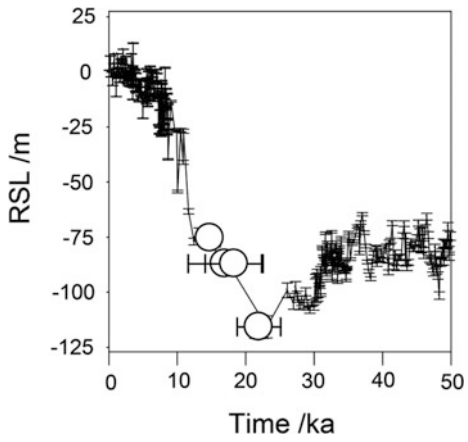

Fig. 9 IRSL SARA ages obtained for the basal unit of core FA13, plotted relative to a sea-level curve for the Red Sea (Grant et al. 2012)

latitude and altitude specific dose rates (0.17 ± 0.01 mGy a^{-1}), with time-dependent corrections for water depth and overburden (for the period the terrestrial sediments accumulated). For the silts sampled in FA6 (0–300 cm depth) and FA13 (0–150 cm depth), the depth of water above the core attenuated the contribution of the cosmic dose rate to a few percent of the total dose. However, for the coarser-grained units sampled at the base of FA13 (from 150 cm depth), consideration was given to the palaeo-environment(s) at the time of deposition; from reconstructions of Red Sea relative sea-levels, it is apparent that the sea flooded rapidly in after deposition of the coarse-grained units, indicating that the cosmic dose contribution needs only to be modeled for a few percent of the total time it could have potentially been accumulating. The net effect of this is that the cosmic dose contribution is very minor relative to the total environmental dose rate at each of the dating positions. Subsequent investigations have shown evidence of excess uranium revealed through analysis of the low energy gamma ray lines from ^{234}Th in comparison with those from further down the decay series. Evidently this is not accompanied by the full decay series, and will be investigated further in future work.

Table 1 lists the IRSL SARA dating results based on the method described above. For core FA6 all data fall into the later part of the Holocene as expected from the profiling results discussed in the previous section. These samples are consistent with sedimentation rates between 0.4 and 1.4 mm a^{-1} with the lowest sample being consistent with a 6 ka marine highstand. For core FA13 the upper part (above 150 cm) covers a similar time interval in the Mid to Late Holocene. At 150 cm, there is a temporal discontinuity, beneath which Late Pleistocene material is encountered. In Fig. 9 the ages obtained from these lower samples have been superimposed on the sea level curve of Grant et al. (2012). Given the water depth of 102 m at time of sampling, the

positioning of the earliest samples on this curve is consistent with a terrestrial Pleistocene environment at the time of deposition.

8 First Evidence for Late Pleistocene Sediments in a Near-Shore Marine Environment in the Red Sea

The cores examined here are the first two appraised out of a collection of 20 recovered offshore at the Farasan Islands by the research cruise of R/V AEGAEO in 2013. The IRSL SARA dates from one of them, core FA13, provides the first evidence so far which confirms that there are surviving fragments of formerly terrestrial palaeo-landscapes preserved under the Red Sea, confirming the hypotheses raised by Bailey et al. in the EFCHED and DISPERSE projects. Furthermore, it has highlighted the value of initial luminescence screening made using portable OSL equipment as an important tool in appraising sediment stratigraphies within cores, offering information on the range and magnitude of the ages recorded in each, and a means to map out and correlate discrete depositional events. The direct evidence from the HCMR cruise and the dating work confirms that such environments are conserved under some marine silts of 1.5 m depth in the position of core FA13. Having conducted both profiling and quantitative methods there appear to be potential for using profiling of similar core materials to generalize the chronology and extend the search for further examples of such environments. This is an important part of the longer-term search for Palaeolithic materials and sites in the nearshore marine environment. While there is a need for further work to replicate these results from other cores to extend the geographic range and to resolve U series behaviour as indicate above, this represents a significant step forward.

9 Analysis and Dating of Sediments Associated with Landscape Evolution and Archaeological Work

The aim of the terrestrial OSL investigations in SW Saudi Arabia was to construct chronologies for sediment stratigraphies in the Jizan and Asir regions and to produce the temporal framework to reconstruct palaeo-environments and -geographies through the Mid Pleistocene and Holocene relative to Palaeolithic migrations and occupations. Three areas were identified for detailed investigations: (1) Wadi Sabiya (Jizan), (2) Dhahaban Quarry (Asir), and (3) Hajambar Quarry (Asir) (Fig. 3c). The significance of sites 1 and 2 is that at each, lithic tools with Middle Stone Age (MSA) affinities were recovered in sediments indirectly dated by association to the Late to Middle Pleistocene. The significance of the third site is that it contains an environmental record, with evidence for a humid phase in the early Quaternary, and thus it is a valuable palaeo-environmental marker for this region.

Robyn Inglis visited the sites in January-February between 2012 and 2015 to collect samples from key units within the sediment stratigraphies for luminescence dating. In the absence of field spectrometry, bulk sediment samples were collected from around each dating position in different geometric schemes to permit reconstruction of the external gamma dose rate from adjacent stratigraphic units (full details are provided for each case study below). In this work, dose rates for the bulk sediment were quantified using HRGS and TSBC in the laboratory coupled with water content analysis. The gamma dose rates for each dating position were determined from the reconciliation of the estimates from the dating position and the adjacent bulk sediment samples. Equivalent dose determinations were obtained, in the first instance, by a quartz OSL SAR method (Murray and Wintle 2000). In some cases, the results go beyond the age limits of quartz saturation. In other cases, issues concerning the interpretation of mixed age dose distributions need to be considered relative to the context of samples, the age limits of the methods, and the association with external age constraints by direct or indirect reference to landscape classification or external information.

Full technical descriptions are provided for each case study in Kinnaird et al. (2015c). In brief, standard sample preparation procedures were used to extract and concentrate sand sized 150–250 μm quartz from each dating sample, the purity of which was checked by scanning electron microscopy, and when impurities or contaminants were noted, these separates were subjected to repeated HCl and HF washes. All measurements were made on the same Risø DA15 OSL/TL readers as described above, but with U340 detection filter packs to detect in the region 270–380 nm. OSL was measured at 125°C for 60 s, integrated over the first 2.4 s of measurement and subtracting an equivalent signal taken from the last 9.6 s. Dose response curves were constructed from 5 to 6 regenerative doses extending up to 200 Gy, or to 500 Gy for those samples whose natural cycle signals exceeded 200 Gy. SAR acceptance checks included recycling and internal dose recovery tests on the dose response curves, zero level checks and IRSL response tests. Aliquots were rejected from further analysis if they failed sensitivity checks (based on test dose response), SAR acceptance checks or where significant IRSL response was associated with anomalous equivalent doses.

Here the outcomes from three sites, Wadi Sabiya, Hajambar Quarry, and Dhahaban Quarry are discussed. The outcomes provide chronological constraints for Late Quaternary environments, including results with MIS3 and MIS5

associations. There are, however, unresolved challenges concerning the extent to which sampling methods can overcome post-depositional influences associated with weathered or reworked elements, and the ability, particularly in coastal marginal settings, of the data themselves to resolve unique parts of the sea level curves associated with the different parts of the glacial cycle. These challenges are discussed at the end of the section.

10 Wadi Sabiya

To the south of Jebel Akwah, 4 km distant, Wadi Sabiya and its tributaries incise wadi floodplain.

Sediments up to 10 m below the surrounding landscape. These deposits are capped by a volcanic tuff which extends for tens of kilometres over the surrounding area. It has been related to the eruption of Jebel Akwah dated by the K-Ar method to 0.44 ± 0.26 Ma (K-Ar; Dabbagh et al. 1984). The Wadi Sabiya has been extensively quarried, revealing thick sedimentary sequences consisting of basal wadi gravel deposits, overlain and cut into by subsequent wadi channel and associated floodplain deposits. Loose blocks of tuff were observed on the very top of the section that had been isolated by quarrying, consistent with but laterally offset to in-situ tuff deposits. On this basis it has been assumed that the sedimentary sequence is overlain by the aforementioned volcanic tuff. The site was visited in January 2014 by Robyn Inglis (Inglis et al. 2014a, b). In the sediment stratigraphy investigated here, the channel deposits contain a worked shale clast, with three long blade removals (potentially the result of soft-hammer percussion, indicative of a MSA technology; Bailey et al. 2015). If this typological assessment is correct, and it is found that the wadi and channel deposits are older than the tuff, then this artefact becomes a contender for the earliest MSA evidence in Arabia given the existing K-Ar dates. To address this, samples were collected for OSL dating from throughout this quarry section, from (i) the silty, fine- to medium-grained, semi-indurated sands which form the fill of the lower channel deposit (SUTL2673), (ii) the finer, sandy silt of the overlying channel deposit (SUTL2672), and (iii) the coarser, sandy silt matrix of the uppermost channel deposit (SUTL2671). The samples were collected with no field spectrometry or portable OSL profiling to characterise the luminescence stratigraphies. However, in addition to the formal dating samples, bulk sediment samples were collected around each of the dating positions, for use in reconstructing the external gamma dose rate. For each position between 18 and 24 dosimetry samples were collected to represent stratigraphic units within 25–30 cm of the dating tube positions.

Dose rates to the dating materials were obtained by HRGS, coupled with beta dose rate measurement using TSBC. To estimate environmental dose rates for the 3 dating tubes examined, composite samples were constructed from the bulk sediments and measured by HRGS, giving effective gamma dose rates between 0.4 and 0.5 mGy a^{-1}. These are comparable with the measured values recorded from dating tubes (0.4–0.5 mGy a^{-1}). Both data sets were combined to estimate the total dose rates for the samples, which ranged from 1.4 and 1.5 mGy a^{-1}. Equivalent doses were determined, initially, by a quartz SAR OSL protocol on 32 aliquots per sample. All samples showed heterogeneity in equivalent dose estimates, with common central tendencies (~35–50 Gy), but with low dose (~10–20 Gy) and high dose (>100 Gy) outliers, leading to some ambiguity in assigning luminescence ages (e.g., Figure 10 (right, a)). Subsequently, 32 additional aliquots per sample were subjected to a simplified two-step SAR protocol to increase the statistical power (e.g., Figure 10 (right, b, c)). For each sample, linear and weighted means and central and common age model estimates of stored dose were indistinguishable between the 32 aliquot and 64 aliquot sets (Fig. 10 (right)). Luminescence ages (Table 2) were calculated using standard microdosimetric models, with uncertainties that combined measurement and fitting errors from the SAR analysis, all dose rate evaluation uncertainties, and allowance for the calibration uncertainties of the sources and reference materials.

The quartz OSL SAR sediment ages obtained from the strata at Wabi Sabiya range between 15 and 29 ka, when weighting the stored dose value toward the low dose component, and 22 and 30 ka, when weighting the stored dose value toward a central tendency. It is clear from the equivalent dose distributions that the majority of quartz aliquots from these sediments are incompatible with the geological expectations, that is, deposition within MIS5 (unless there are other mechanisms for reworking or partially resetting the OSL signals in these sections after deposition). This raises questions about the assumed stratigraphic relationship between these wadi deposits and the potentially overlying tuffs, as well as the post-depositional history of the sediments. It would take further fieldwork and investigations to resolve these questions.

11 Hajambar Quarry

A quarry 10 km northwest of Hajambar (Fig. 3c), adjacent to the road connecting Al Haridhah and Al Edati, was identified as containing wadi deposits overlying a lava flow. The quarry is approximately 15 m deep, and 100 m wide. The top of the sequence is at ~30 m asl. A reconnaissance visit in June 2012 identified laminated silts and grits at the base of the quarry, interpreted as wadi overbank deposits, laid down during a humid phase and potentially providing a

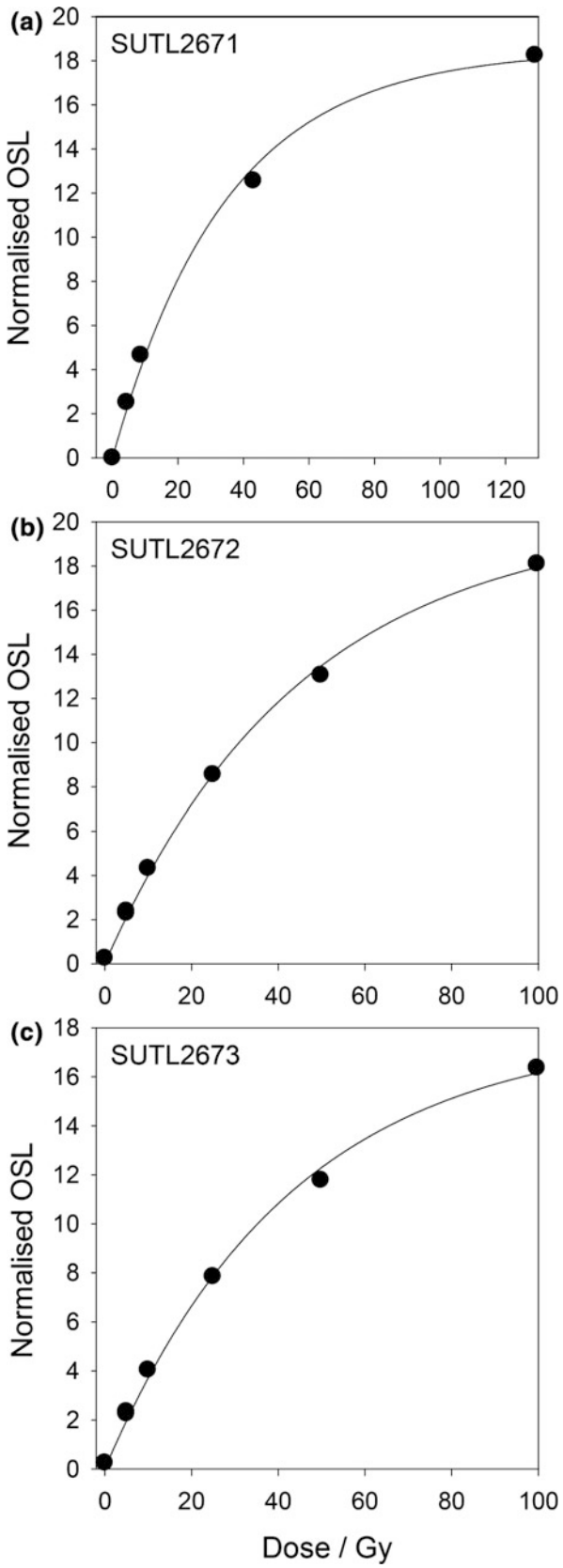

Fig. 10 Illustrative dose response curves (left hand figures) from quartz SAR-OSL determinations from Wadi Sabiya, and (right hand side) dose distributional plots. It is notable that the dose distributions observed for the **a** 32 aliquot and **b** and **c** 64 aliquot sets are indistinguishable within the limits of error; although over-dispersion is emphasised in the latter

Table 2 Luminescence ages for the sediments sampled at Wadi Sabiya

Sutl no.		Weighted mean		Central dose model	
	Dose rate (mGy a^{-1})	Stored dose (Gy)	Age (ka)	Stored dose (Gy)	Age (ka)
2671	1.40 ± 0.08	21.8 ± 1.3	15.5 ± 1.3	37.3 ± 2.8	26.6 ± 2.4
2672	1.50 ± 0.08	22.3 ± 0.7	14.9 ± 0.9	32.1 ± 2.4	21.5 ± 1.9
2673	1.35 ± 0.07	39.1 ± 1.1	29.0 ± 1.8	40.7 ± 2.4	30.0 ± 2.4

rare palaeoenvironmental marker from SW Arabia. These deposits are overlain by a silty sand unit dominated by rhyzoliths and carbonate concretions. The quarry section is cut by a number of faults and fractures, which offset the sediments, and have also acted as conduits for fluid movement and precipitation of carbonates. These were logged and sampled in November 2012 (Bailey et al. 2012) for micromorphological and sedimentological analysis, and three tubes were taken for OSL dating (SUTL2805-07). The site was revisited in February 2014 to collect further OSL samples (Inglis et al. 2014b). This later visit was complicated by the partial flooding of the quarry, with water covering the base of the sediments sampled in 2012 and the trench dug below. It is possible that the water had, at some point in the very recent past, covered the laminated sediments. Two OSL samples and background samples were taken from the upper part of the laminated silts (SUTL2808-09). In stark contrast to conditions in 2012 when the sections were completely dry, the sediments were wet in 2014 at time of sampling. In addition to the formal dating samples, single composite bulk sediment samples were collected around each of the 2012 samples, with sets of 18 bulk samples from within 0–30 cm of the 2014 samples, to reconstruct the external gamma dose rate.

These sediments were dated using the combination of equivalent dose determinations by quartz SAR OSL, coupled with dose rate determinations using the combination of HRGS and TSBC. Composite sediment samples were constructed using the bulk surrounding each dating position at spacings of 0–8 cm, 8–15 cm, and 15–25 cm. To estimate environmental dose rates for the 2014 dating tubes examined, composite samples were constructed from the bulk sediments and measured by HRGS, giving effective gamma dose rates between 0.3 and 0.5 mGy a^{-1}. These are comparable with the measured values recorded from dating tubes (0.4–0.6 mGy a^{-1}). Both data sets were combined to estimate the total dose rates for the samples, which ranged from 0.9–1.7 mGy a^{-1}. 16 aliquots of quartz were prepared for each sample and analysed by the quartz OSL SAR method. The data derived from the SAR dose determinations were analysed at two scales; composite data sets were explored using Excel spreadsheets and Jandel Sigmaplot software, while individual dose response curves were analysed using the Risø 'Analyst' program. Individual decay curves were scrutinised for shape and signal consistency, and compared relative to other aliquots in their 16 aliquot and preheat set. Individual (aliquot-specific) dose response curves were determined using an exponential fit. Only one produced a finite age (SUTL2805; Fig. 11), although with considerable scatter in its equivalent dose distribution, indicating some mixing of materials with residual ages. The remaining four samples showed natural luminescence signals in excess of the saturation signals for the regenerative dose curves. In an attempt to extract age data from the two remaining samples, additional regenerative dose points were added up to a nominal 500 Gy; for one of these samples (SUTL2809), a slight increase in individual normalised dose response was noted; however, for the second of these (SUTL2808), the individual normalised dose responses showed no additional growth.

The uppermost sample in the quarry (SUTL 2805; Fig. 11) yielded an age estimate of approximately 110 ka (Table 3), with weighted standard deviation across the equivalent dose distribution (30 ka) and the weighted standard error (10 ka) indicated. The lower samples in the quarry face did not yield finite ages. For two of these samples, a number of individual aliquots did yield natural normalised signals within the limits of their respective regenerative dose curves, suggesting sediment ages in excess of >90 ka (SUTL2806) and in excess of >55 ka (SUTL2807). Minimum age estimates for the lower strata are in excess of >120 ka. Notwithstanding the limitations of the Hajambar quartz, which saturates early, the quartz OSL SAR data do provide a temporal constraint to the end of the humid phase based on the upper two samples on the environmental section of some 90–100 ka. Since the quartz OSL signals from the majority of samples are in saturation there would be scope for exploring age extension methods in the future work if finite age estimates for these deposits are required.

12 Dhahaban Quarry

A quarry 3 km south of Dhahaban (Fig. 3c), adjacent to the coastal road connecting Hajambar and Dhahaban, was selected for study following the discovery of abundant surface lithics (>700 in number), as well as lithics embedded with the sediments (Bailey et al. 2015; Inglis et al. 2014a).

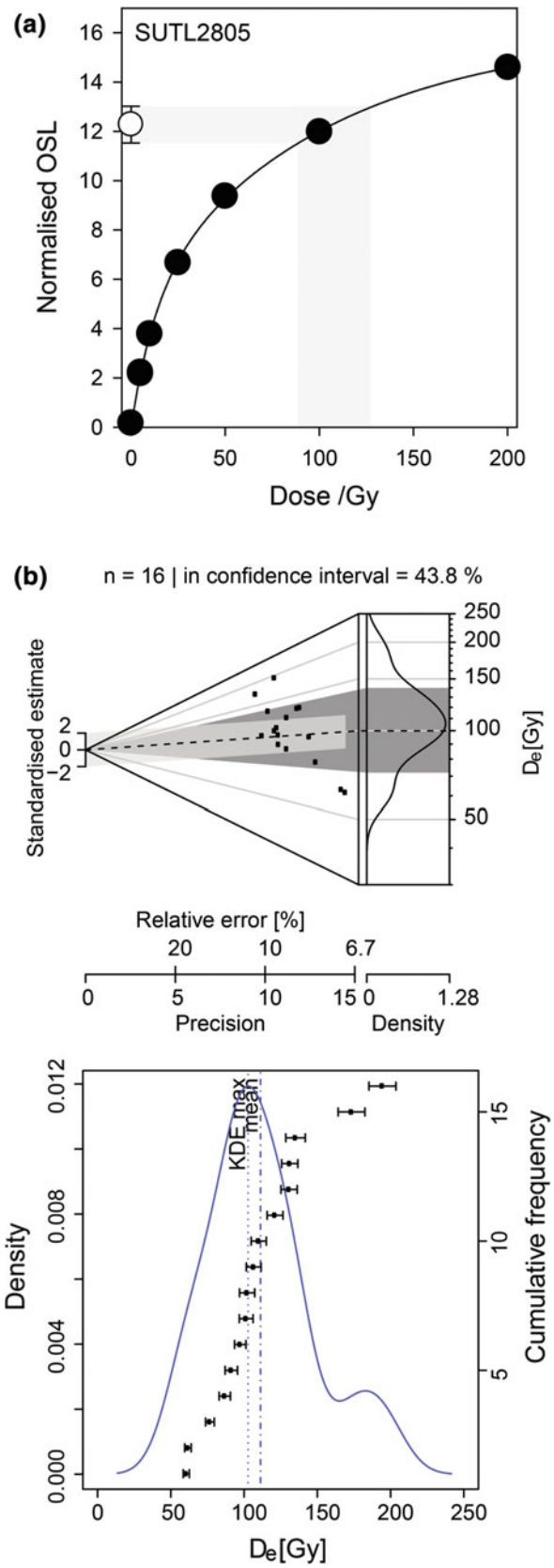

Fig. 11 Dose response curve and dose distributions from sample SUTL2805 from Hajambar, leading to a finite quartz SAR OSL age within MIS5

Table 3 Luminescence ages for the sediments sampled at Hajambar quarry

Sutl no.	Dose rate (mGy a^{-1})	Stored dose (Gy)	Age (ka)
2805	0.94 ± 0.04	100 ± 25 (7)	110 ±30 (10)
2806	1.01 ± 0.04	>90 Gy	>90
2807	1.58 ± 0.05	>50–55 Gy	>30
2808	1.06 ± 0.04	>200–250 Gy	>120–150
2809	1.15 ± 0.04	>150 Gy	>130

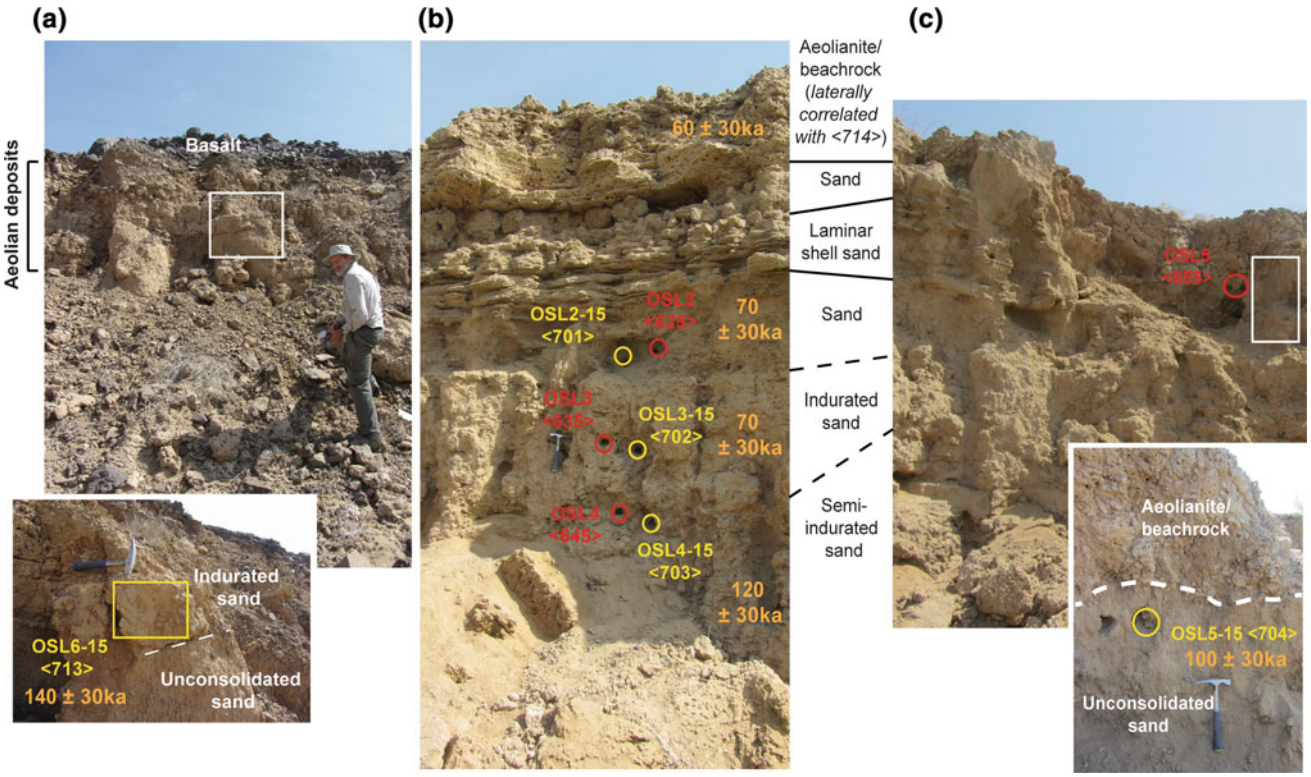

Fig. 12 The stratigraphy at Dhahaban quarry and positions of samples gathered in 2014 (red symbols) and 2015 (yellow symbols) together with the age determinations from the later series of analyses. Samples were collected in three parts of the quarry labelled a, b and c below, with additional cutting back between the 2014 and 2015 sampling

The deposits at the Dhahaban Quarry site comprise a basal wadi cobble unit (restricted to one area and containing 19 andesite artefacts with MSA affinities), overlain by coral terraces and shallow marine sediments in different parts of the locality, the latter capped by beachrock and aeolianites (Inglis et al., this volume). The upper surfaces of the marine/beach deposits are ~6 m asl, and the complex overlies a degraded, westward dipping, basalt slope. A ~6 m deep section in the main quarry area sampled for OSL analysis comprised (from the base up): (1) a 50 cm-thick, semi-indurated fine- to medium-grained sand, with laminae of coarser sands; (2) approximately 70 cm thick, indurated medium-grained sands, containing marine shells; (3) about 50 cm of unconsolidated sands; (4) about 170 cm of laminated consolidated, shell-dominated sands grading into more poorly consolidated sands; and (5) the capping aeolianite. The site was visited in reconnaissance in 2012, then again in 2014, for more systematic geomorphological mapping and archaeological surveying (Inglis et al. 2014b). The section was first sampled for OSL in 2014, with 4 samples taken from two locations within the quarry; units in the main marine quarry sedimentary stratigraphy were sampled three times across in two locations ~40 m laterally offset along the main cut (Fig. 12a, b); the fourth sample was removed from 100 m E of the quarry section, the aeolianite overlying the basalt jebel (Fig. 12c).

Following preliminary OSL analyses, outlined below, which produced age estimates which were systematically

younger than expected, the sections were re-sampled in 2015 with further cleaning and cutback (Inglis et al. 2015). Samples were taken to date deposition of the shallow marine deposits within the raised beach complex (SUTL2674-76 and SUTL2810-13) to provide age estimates of the high sea stand in this part of the Red Sea and terminus ante quem (TAQ) estimates for deposition of the unit containing stratified MSA lithics. Additional samples were collected from the aeolianites capping the sequence (SUTL2677 and SUTL2814-15).

The samples collected in 2014 were subjected to OSL analyses in 2015 (prior to the re-visit of the site that year). The outcomes were younger than expected on geomorphological grounds, ranging from 25–40 ka, depending on which dose distributional model was favoured, but all from periods when sea level was expected to be very much lower than contemporary settings or former Quaternary high stands. This raised questions concerning sample integrity and the extent to which potential weathering, bleaching or thermal signal erosion prior to collection might have led to underestimation of the original depositional ages. The subsequent set of samples were cut back further, although for the indurated sands there were limits to what was practical in the field, and it may be necessary to return for further sampling with mechanical cut-backs to ensure that surface alteration has been overcome. Ages were obtained using separated quartz SAR OSL analysis, coupled with dose rate analysis by HRGS and TSBC. Given the close association between the 2014 and 2015 samples, the gamma dose rates measured by HRGS for the paired sets were reconciled in a dosimetric model. This yielded effective gamma dose rates between 0.4 and 0.5 mGy a^{-1}, indistinguishable from those measured directly on the dating materials (0.4–0.5 mGy a^{-1}). Total effective dose rates for the 2015 samples ranged between 1.0–1.5 mGy a^{-1}, comparable to those obtained in 2014, which varied over the same range. Equivalent dose determinations were made using 16 small aliquots per sample. All samples showed heterogeneous dose distributions, with common central tendencies (>60 Gy), but with both low dose (30–80 Gy) and high dose (100–180 Gy) components (outliers at 2σ). Also, for some samples, individual aliquots returned normalised natural OSL signals above the saturation limits of their dose response curve. For each sample, different dose components were modelled with respect to the elevation of the raised beach complex, the expected age of the marine terrace, and the required uplift rates (calculated with respect to the present elevation and the potential age of the terrace). In comparison with the results from the 2014 samples, quartz SAR OSL ages for the marine sediments fall in the range 120 ± 40 ka to 50 ± 20 ka, for SUTL2812 and 2811 respectively, and for the aeolianites, 90 ± 30 ka to 60 ± 30 ka, for SUTL2813 and 2815 respectively (Table 4).

The fossil beach complex overlies (in part) a wadi cobble unit containing stratified lithics with Middle Stone Age affinities; the sediment ages for the terrace provide a TAQ for cultural activity in this area from 120 ka.

While these data have extended the estimated ages of the Dhahaban units back to early parts of the glacial cycle including MIS5 and provide a general link to the Middle Palaeolithic artefacts obtained from the area, there are still difficulties in reconciling the sample stratigraphy, the heterogeneous dose distributions and sedimentary sequence within reconstructed sea level histories which need to be given further attention in future work. The difficulties are illustrated in Figs. 13 and 14. Taking the sea level curves of Grant et al. (2012), Fig. 13 identifies the times in the past 150 ka when sea levels would have been within range, under a series of uplift scenarios (as average rates), to position coastal material in the current location (Wilson et al. 2014). This indicates that three parts of MIS5 might have been associated with near-coastline positions at (a) 80–88 ka (MIS5a–b), (b) 100–110 ka (MIS5 c–d), and (c) 120–135 ka (MIS5e and before), with mean uplift rates of 0.5, 0.2 and 0 mm/a. It is instructive to consider how the data fall relative to these potential periods for possible deposition.

This is shown in Fig. 14 for the three marine samples at the base of the section. The coloured bands on the figure indicate the three uplift scenarios within MIS5 which could potentially provide plausible periods for deposition of sediments in this location. Clearly there are aliquots within each sample which fall both above and below the shaded areas, and at this stage the data sets do not provide an indication of a unique assignment to one of the three uplift scenarios. The

Table 4 Luminescence ages for the sediments sampled at Dhahaban quarry

Sutl no.	Dose rate (mGy a^{-1})	Stored dose (Gy)	Age (ka)
2810	1.50 ± 0.07	109 ± 45 (14)	70 ± 30 (10)
2811	1.26 ± 0.06	86 ± 33 (9)	70 ± 30 (10)
2812	1.33 ± 0.06	153 ± 45 (17)	120 ±30 (15)
2813	1.49 ± 0.05	143 ± 38 (17)	100 ±30 (10)
2814	1.04 ± 0.06	145 ± 68 (26)	140 ±70 (30)
2815	1.09 ± 0.07	64 ± 30 (9)	60 ± 30 (10)

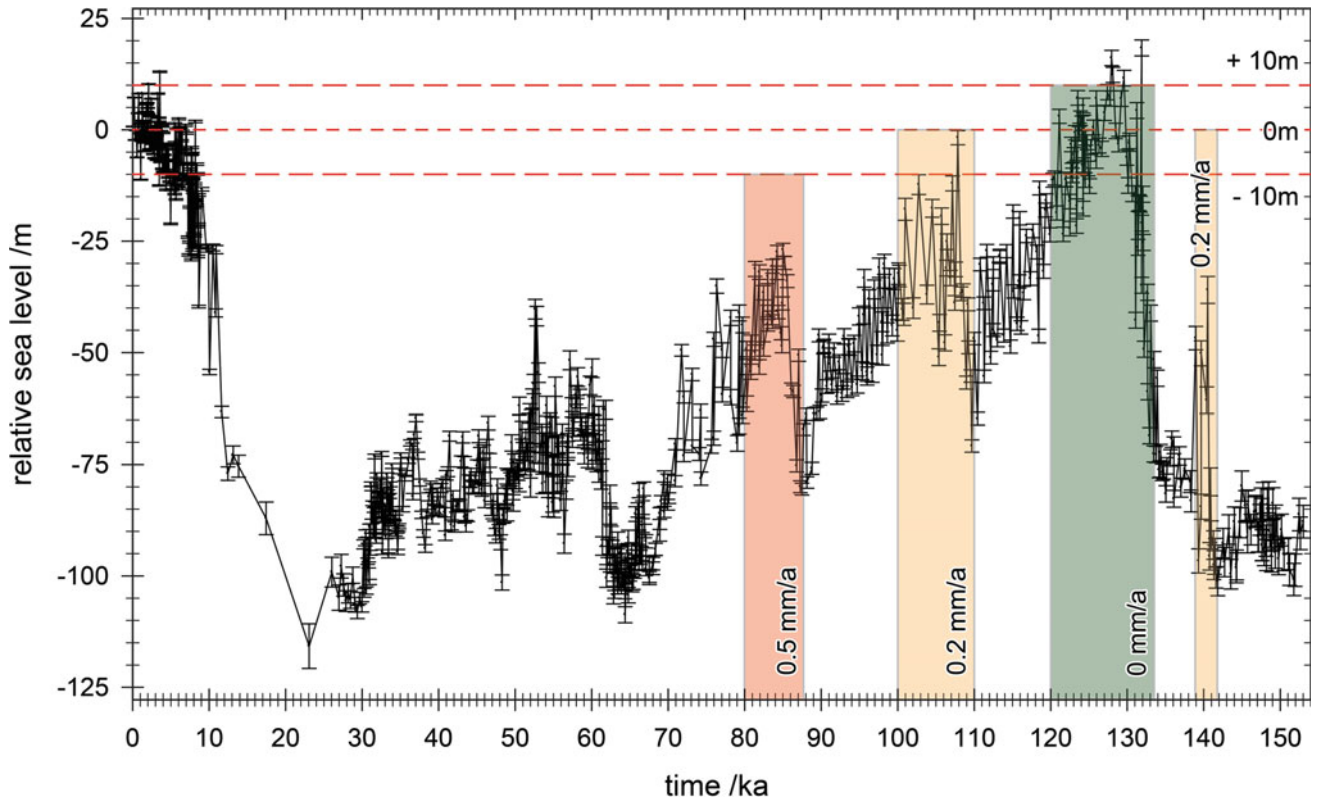

Fig. 13 Relative sea level curve for the Red Sea Region (Grant et al. 2012), annotated with the approximate uplift rates necessary to place the Dhahaban fossil beach complex at its present position assuming different luminescence depositional ages

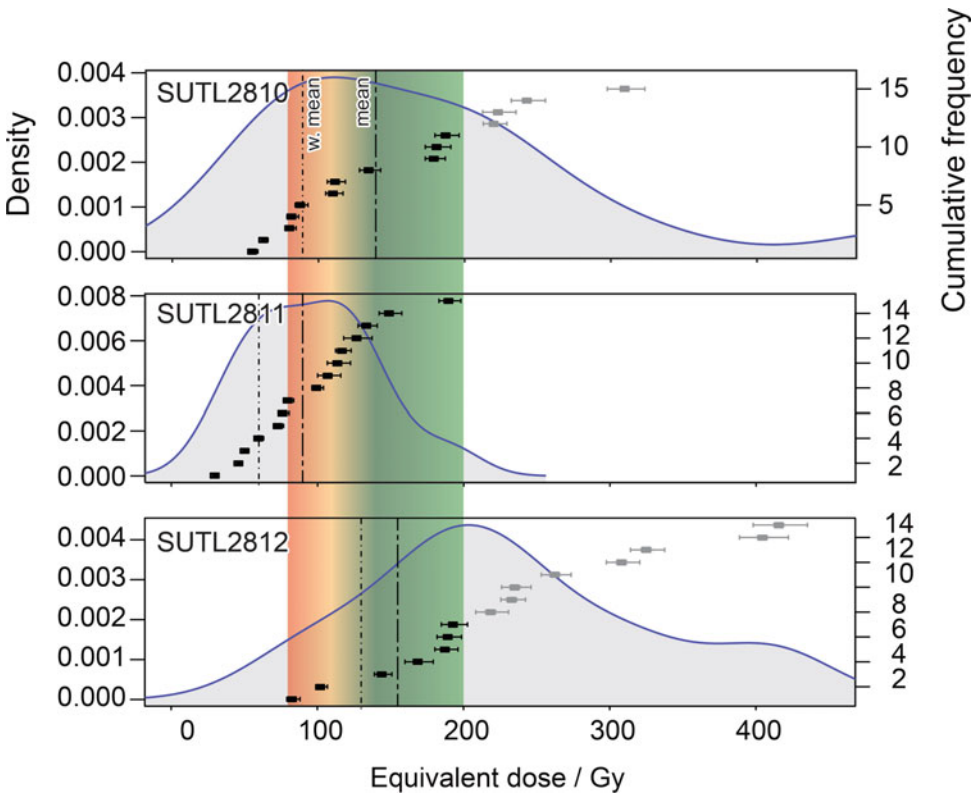

Fig. 14 KPE plots (after Dietze et al. 2013) for SUTL2810–2812, the marine sediments at the base of the section superimposed on the uplift scenarios of Fig. 13

central dose estimates for SUTL2810 span the youngest and oldest plausible MIS stage 5 possibilities, depending on whether weighted or non-weighted analyses are preferred. For sample SUTL2811 only the unweighted estimate falls within a plausible period, and would require the highest uplift rate considered (0.5 mm a^{-1}). Only for sample SUTL2810 do both weighted and unweighted estimates fall within MIS5e, which might be considered the scenario which is most consistent with current estimates of uplift rate in the region (cf., Lambeck et al. 2011; Pedoja et al. 2014, and references therein). Even there it is clear that some aliquots tail to higher doses raising the possibility that earlier Quaternary high stand cycles, beyond the range of the quartz SAR method, may also need to be considered in future work. This site, which has important Palaeolithic associations and a stratigraphy which implies several cycles of induration and sedimentation, appears therefore at this stage to raise several possible scenarios relative to coastal processes and humidity cycles. While the second sampling campaign resulted in earlier central age estimates and makes MIS5 attributions plausible, challenges remain to eliminate any remaining limitations associated with sampling and to achieve a chronology which can separate the specific MIS stage from the plausible candidates listed above, and perhaps from earlier Quaternary highstands. To our knowledge this is challenging too for other dating methods, and it would seem that additional field and laboratory studies are needed to resolve the limitations of current data sets in these important landscapes.

13 Discussion and Implications for Future Research

As indicated in this chapter there is emerging evidence from sediment dating studies in the terrestrial environment for cycles of humidity and aridity going back to at least 200–300 ka. This sets an important series of challenges to ongoing research in the region. Current methods have the capacity to work within the timeframe up to 200–300 ka and, with new developments, to perhaps extend it to earlier Quaternary periods. However, new work will be needed both on method development and validation and on identification, detailed sampling and analysis of such earlier Quaternary units in order to refine chronologies for landscape and palaeoenvironmental evolution studies. Coupling of the Arabian and Red Sea environments to the monsoon cycle and the African aridity cycle is also an area for future development, and the Red Sea region is potentially an important interface zone for such studies. In this chapter, work associated with the DISPERSE project has also been presented in both near-shore marine settings and in terrestrial settings. Linking the results of direct sediment analyses and chronologies to current knowledge of sea level history during the last glacial cycles is both important to setting the palaeoenvironmental context for human dispersal and current archaeological exploration.

In the marine application presented here the utility of luminescence profiling has been clearly demonstrated as a new and critical part of the search for Late Pleistocene sediments with terrestrial associations in today's marine environments. The case illustrated of the Farasan core FA13, which has an erosional discontinuity below which Late Pleistocene material survives from the end of the last glacial cycle in a contemporary sea water depth of 80 m, shows the combined utility of both profiling and luminescence dating. It provides the first concrete verification of the long-searched-for evidence that this part of the Red Sea margin contains the predicted environments where the search for Palaeolithic material in former littoral fringes can be conducted. The other case studies presented here, in association with DISPERSE, are related to the ongoing search for landscapes and sites associated with Palaeolithic archaeology and associated palaeo-landscapes in terrestrial settings. The examples presented include former water-lain sediments at Wadi Sabiya, Hajambar and Dhahaban, with palaeoenviromental and archaeological significance. Results obtained so far at these sites span a period from 20 ka up to >150 ka, based on quartz SAR dating. At this stage, there are outstanding questions concerning the extent to which sampling cut-backs of the older units are needed to overcome post-depositional alteration and potential thermal erosion of signals from earlier Quaternary periods. In the case of the older units such as those at Hajambar, and potentially at Dhahaban, age extension work may be needed to push the age limits back to and beyond MIS5e. There is more work needed to refine chronologies sufficiently to provide unique separation of some of the subdivisions of MIS5, which are of critical importance to materials in the littoral fringes of the Red Sea. But notwithstanding those future challenges, it is quite clear the luminescence dating is making important contributions to understanding the environments of the Red Sea.

Acknowledgements The work presented in the section on luminescence dating and DISPERSE was supported by ERC Advanced Grant 269586 DISPERSE (Dynamic Landscapes, Coastal Environments and Hominin Dispersals) and by the Saudi Commission for Tourism and National Heritage (SCTH) through its President, Prince Sultan bin Salman bin Abdul Aziz, and his staff. The support, involvement and contributions from Prof. Geoff Bailey, Dr. Dimitris Sakellariou and Dr. Robyn Inglis are gratefully acknowledged. Dr. Alan Cresswell, Dr. Lorna Carmichael and Mr. Simon Murphy are also acknowledged for their help in the laboratory. The work presented here formed an invited presentation at the Jeddah workshop on the Geological Setting, Oceanography and Environment of the Red Sea, held in February 2016. We would like to thank the Saudi Geological Survey, and particularly Dr. Najeeb Rasul, for hosting this workshop and supporting the publication. This is DISPERSE contribution no. 44.

References

Adamiec G, Bailey RM, Wang XL, Wintle AG (2008) The mechanism of thermally transferred optically stimulated luminescence in quartz. J Phys D: Appl Phys 41:135503–135517

Adamiec G, Duller GAT, Roberts HM, Wintle AG (2010) Improving the TT-OSL SAR protocol through source trap characterization. Radiat Meas 45:768–777

Aitken MJ (1985) Thermoluminescence dating. Academic Press, London

Aitken MJ (1998) An introduction to optical dating: The dating of Quaternary sediments by the use of photon-stimulated luminescence. Oxford Science Publications, Oxford

Alexander SA (2007) The stability of the remnant luminescence emissions of alkali feldspar. Ph.D. Thesis, University of Glasgow. http://theses.gla.ac.uk/1001/

Armitage SJ, Jasim SA, Marks AE, Parker AG, Usik VI, Uerpmann H-P (2011) The southern route "Out of Africa": Evidence for an early expansion of modern humans into Arabia. Science 331:453–456

Bailey GN, Flemming NC, King GCP, Lambeck K, Momber G, Moran LJ, Al-Sharekh A, Vita-Finzi C (2007) Coastlines, submerged landscapes and human evolution: The Red Sea Basin and the Farasan Islands. J Isl Coast Archaeol 2:127–160

Bailey GN, Flemming NC (2008) Archaeology of the continental shelf: Marine resources, submerged landscapes and underwater archaeology. Quat Sci Rev 27:2153–2165

Bailey GN, King GCP (2011) Dynamic landscapes and human dispersal patterns: Tectonics, coastlines and reconstruction of human habitats. Quaternary Sci Rev 30:1533–1553

Bailey GN, Inglis RH, Meredith-Williams MG, Hausmann NBMJ, Alsharekh AM, Al Ghamdi S (2012) Preliminary Report on Fieldwork in the Farasan Islands and Jizan Province by the DISPERSE Project. November-December 2012. University of York/Saudi Commission for Tourism and Antiquities. http://eprints.whiterose.ac.uk/80966/

Bailey GN, Devès MH, Inglis RH, Meredith-Williams MG, Momber G, Sakellariou D, Sinclair AGM, Rousakis G, Al Ghamdi S, Alsharekh AM (2015) Blue Arabia: Palaeolithic and underwater survey in SW Saudi Arabia and the role of coasts in Pleistocene dispersals. Quat Int 382:42–57

Blechschmidt I, Matter A, Preusser F, Rieke-Zapp D (2009) Monsoon triggered formation of Quaternary alluvial megafans in the interior of Oman. Geomorphology 110:128–139

Bøtter-Jensen L, Bulur E, Duller GAT, Murray AS (2000) Advances in luminescence instrument systems. Radiat Meas 32:523–528

Boulton GS (1993) Ice ages and climate. In: Duff PMcLD (ed) Holmes Principles of physical geology, 4th edn. Chapman and Hall, London, pp 439–469

Bray HE, Stokes S (2003) Chronologies for Late Quaternary barchan dune reactivation in the southeastern Arabian Peninsula. Quaternary Sci Rev 22:1027–1033

Bray HE, Stokes S (2004) Temporal patterns of arid-humid transitions in the south-eastern Arabian Peninsula based on optical dating. Geomorphology 59:271–280

Breeze PS, Drake NA, Groucutt HS, Parton A, Jennings RP, White TS, Clark-Balzan L, Shipton C, Scerri EML, Stimpson CM, Crassard R, Hilbert Y, Alsharekh A, Al-Omari A, Petraglia MD (2015) Remote sensing and GIS techniques for reconstructing Arabian palaeohydrology and identifying archaeological sites. Quatern Int 382:98–119

Burbidge CI, Sanderson DCW, Fülöp R (2007a) Luminescence dating of dune sand, wadi, sabkha and playa sediments, Saudi Arabia. Technical Report, SUERC, 120 pp. http://eprints.gla.ac.uk/76538/

Burbidge CI, Sanderson DCW Housley RA, Jones P (2007b) Survey of Palaeolithic sites by luminescence profiling; a case study in eastern Europe. Quaternary Geochronology 2:296–302

Burns SJ, Matter A, Frank N, Mangani A (1998) Speleothem based paleoclimatic record from northern Oman. Geology 26:499–502

Buylaert JP, Murray AS, Thomsen KJ, Jain M (2009) Testing the potential of an elevated temperature IRSL signal from K-feldspar. Radiat Meas 44:560–565

Cresswell AC, Sanderson DCW (2009) Luminescence dating of dune sands and sabkha sediments in Saudi Arabia. SUERC dating report, SUERC, p 37

Dabbagh AR, Emmermann H, Hötzl AR, Jado HJ, Lippolt W, Kollman H, Moser W, Rauert ZJ (1984) The development of Tihamat Asir during the Quaternary. In: Jado AR, Zötl JG (eds) Quaternary Period in Saudi Arabia, vol 2. Sedimentological, Hydrogeological, Hydrochemical, Geomorphological. Geochronological and Climatological Investigations in Western Saudi Arabia. Springer-Verlag, Vienna, pp 150–173

Dennell R, Petraglia MD (2012) The dispersal of Homo sapiens across southern Asia: How early, how often, how complex? Quaternary Sci Rev 47:15–22

Dietze M, Kreutzer S, Fuchs MC, Burow C, Fischer M, Schmidt C (2013) A practical guide to the R package Luminescence. Ancient TL 32:11–18

Duller GAT (2016) Challenges involved in obtaining luminescence ages for long records of aridity: Examples from the Arabian Peninsula. Quatern Int 410:69–74

Farrant AR, Duller GAT, Parker AG, Roberts HM, Parton A, Knox RWO, Bide T (2015) Developing a framework of Quaternary dune accumulation in the northern Rub' al-Khali, Arabia. Quatern Int 382:132–144

Glennie KW, Singhvi AK (2002) Event stratigraphy, paleoenvironment and chronology of SE Arabian deserts. Quaternary Sci Rev 21:853–869

Glennie K, Fryberger S, Hern C, Lancaster N, Teller J, Pandey V, Singhvi A (2011) Geological importance of luminescence dates in Oman and the Emirates: An overview. Geochronometria 38:259–271

Grant KM, Rohling EJ, Bar-Matthews M, Ayalon A, Medina-Elizalde M, Ramsey CB, Satow C, Roberts AP (2012) Rapid coupling between ice volume and polar temperature over the past 150,000 years. Nature 491:744–747

Groucutt HS, Scerri EML, Lewis L, Clark-Balzan L, Blinkhorn J, Jennings RP, Parton A, Petraglia MD (2015a) Stone tool assemblages and models for the dispersal of Homo sapiens out of Africa. Quaternary International 382:8–30

Groucutt HS, Shipton C, Alsharekh A, Jennings R, Scerri EML, Petraglia MD (2015b) Late Pleistocene lakeshore settlement in northern Arabia: Middle Palaeolithic technology from Jebel Katefeh, Jubbah. Quaternary International 382:215–236

Groucutt HS, White TS, Clark-Balzan L, Parton A, Crassard R, Jennings RP, Parker AG, Breeze PS, Scerri EML, Alsharekh A, Petraglia MD (2015c) Human occupation of the Arabian Empty Quarter during MIS 5: Evidence from Mundafan Al-Buhayrah, Saudi Arabia. Quaternary Sci Rev 119:116–135

Hausmann N, Meredith-Williams M (2016) Seasonal patterns of coastal exploitation on the Farasan Islands. J Island Coastal Archaeology, Saudi Arabia. https://doi.org/10.1080/15564894.2016.1216478

Hilbert YH, Parton A, Morley MW, Linnenlucke LP, Jacobs Z, Clark-Balzan L, Roberts RG, Galletti CS, Schwenninger JL, Rose JI (2015) Terminal Pleistocene and Early Holocene archaeology and stratigraphy of the southern Nejd, Oman. Quatern Int 382:250–263

Hoffmann G, Rupprechter M, Rahn M, Preusser F (2015) Fluvio-lacustrine deposits reveal precipitation pattern in SE Arabia during early MIS 3. Quatern Int 382:145–153

Huntley DJ, Godfrey-Smith DI, Thewalt MLW (1985) Optical dating of sediments. Nature 313:105–107

Inglis RH, Sinclair A, Shuttleworth A, Alsharekh A, Al Ghamdi S, Devès M (2014a) Investigating the Palaeolithic landscapes and

archaeology of the Jizan and Asir regions, southwest Arabia. Proc Seminar for Arabian Studies 44:193–212

Inglis RH, Sinclair AGM, Shuttleworth A, Meredith-Williams MG, Hausmann N, Budd W, Alsharekh A, Al Ghamdi S, Bailey GN (2014b) Preliminary Report on 2014 Fieldwork in Southwest Saudi Arabia by the DISPERSE project: (1) Jizan and Asir Provinces. University of York/Saudi Commission for Tourism and Antiquities. http://eprints.whiterose.ac.uk/80965/

Inglis RH, Foulds F, Shuttleworth A, Alsharekh AM, Al Ghamdi S, Sinclair AG, Bailey GN (2015) The Palaeolithic Occupation of the Harrat Al Birk: Preliminary Report on the 2015 Fieldwork in Asir Province, Southwest Saudi Arabia. University of York/Saudi Commission for Tourism and Antiquities. http://eprints.whiterose.ac.uk/84382/

Jennings RP, Shipton C, Breeze P, Cuthbertson P, Bernal MA, Wedage WMCO, Drake NA, White TS, Groucutt HS, Parton A, Clark-Balzan L, Stimpson C, al Omari A-A, Alsharekh A, Petraglia MD (2015a) Multi-scale Acheulean landscape survey in the Arabian Desert. Quaternary International 382:58–81

Jennings RP, Singarayer J, Stone EJ, Krebs-Kanzow U, Khon V, Nisancioglu KH, Pfeiffer M, Zhang X, Parker A, Parton A, Groucutt HS, White TS, Drake NA, Petraglia MD (2015b) The greening of Arabia: Multiple opportunities for human occupation of the Arabian Peninsula during the Late Pleistocene inferred from an ensemble of climate model simulations. Quatern Int 382:181–199

Kinnaird TC, Cresswell AJ, Bishop P, Sanderson DCW (2010) Luminescence Dating of Samples from Raised Beaches in Tanzania. Technical Report SUERC. http://eprints.gla.ac.uk/76481/

Kinnaird TC, Sanderson DCW, Bigelow GF (2015a) Feldspar SARA IRSL dating of very low dose rate aeolian sands from Sandwick South, Unst, Shetland. Quat Geochronol 30:168–174

Kinnaird TC, Sanderson DCW, Sakellariou D, Bailey G (2015b) Palaeographic reconstructions of the submerged prehistoric landscapes of the Farasan continental shelf, South Red Sea: Chronological constraints. Technical Report, SUERC, 49 pp. http://eprints.gla.ac.uk/110542/

Kinnaird TC, Sanderson DCW, Inglis R, Bailey G (2015c) OSL dating of terrestrial sediments from SW Saudi Arabia: Wadi Sabiya (Jirzan region) and Harrat Al Birk (Asir region). Technical Report, SUERC, 56 pp. http://eprints.gla.ac.uk/110550/

Lambeck K, Purcell A, Flemming NC, Vita-Finzi C, Alsharekh AM, Bailey GN (2011) Sea level and shoreline reconstructions for the Red Sea: Isostatic and tectonic considerations and implications for hominin migration out of Africa. Quaternary Sci Rev 30:3542–3574

Lancaster N, Wolfe S, Thomas D, Bristow C, Bubenzer O, Burrough S, Duller G, Halfen A, Hesse P, Roskin J, Singhvi A, Tsoar H, Tripaldi A, Yang X, Zárate M (2016) The INQUA Dunes Atlas chronologic database. Quatern Int 410:3–10

Matter A, Neubert E, Preusser F, Rosenberg T, Al-Wagdani K (2015) Palaeo-environmental implications derived from lake and sabkha deposits of the southern Rub' al-Khali, Saudi Arabia and Oman. Quatern Int 382:120–131

McClure HA (1976) Radiocarbon chronology of Late Quaternary lakes in the Arabian Desert. Nature 263:755–756

McDougall DJ (1968) (ed) Thermoluminescence of geological materials. Academic, New York

McLaren SJ, Al-Juaidi F, Bateman MD, Millington AC (2009) First evidence for episodic flooding events in the arid interior of central Saudi Arabia over the last 60 ka. J Quaternary Sci 24:198–207

Munro RN, Wilkinson TJ (2007) Environment, landscapes and archaeology of the Yemeni Tihamah. In: Starkey J, Starkey P, Wilkinson T (eds) Natural Resources and Cultural Connections of the Red Sea. British Archaeological Reports International Series 1661. Archaeo Press, Oxford, pp 13–33

Munro RN, Walkington H, Franks S, Wilkinson TJ, Sanderson DCW (2013) Aspects of Late Cainozoic aeolian landscapes in Arabia: Implications for early man. In: Al Ansary AR, Al-Muaikei KI, Alsharekh AM (eds) Man and Environment in the Arab World in Light of Archaeological Discoveries. Abdul Rahman Al-Sudairy Foundation, Riyadh, pp 7–46. ISBN 978-603-90326 5-6

Murray AS, Wintle AG (2000) Luminescence dating of quartz using an improved single-aliquot regenerative-dose protocol. Radiat Meas 32:57–73

Parton A, Farrant AR, Leng MJ, Telfer MW, Groucutt HS, Petraglia MD, Parker AG (2015a) Alluvial fan records from southeast Arabia reveal multiple windows for human dispersal. Geology 43:295–298

Parton A, White TS, Parker AG, Breeze PS, Jennings R, Groucutt HS, Petraglia MD (2015b) Orbital-scale climate variability in Arabia as a potential motor for human dispersals. Quatern Int 382:82–97

Pedoja K, Husson L, Johnson ME, Melnick D, Witt C, Pochat S, Nexer M, Delcaillau B, Pinegina T, Poprawski Y, Authemayou C, Elliot M, Regard V, Garestier F (2014) Coastal staircase sequences reflecting sea-level oscillations and tectonic uplift during the Quaternary and Neogene. Earth-Sci Rev 132:13–38

Petit-Maire N, Carbonel P, Reyss JL, Sanlaville P, Abed A, Bourrouillh R, Fontugne M, Yasin S (2010) A vast Eemian palaeolake in southern Jordan (29 N). Global Planet Change 72:368–373

Petraglia MD (2011) Archaeology: Trailblazers across Arabia. Nature 470:50–51

Petraglia MD, Alsharekh AM, Crassard R, Drake NA, Groucutt H, Parker AG, Roberts RG (2011) Middle Paleolithic occupation on a Marine Isotope Stage 5 lakeshore in the Nefud Desert, Saudi Arabia. Quaternary Sci Rev 30:1555–1559

Petraglia MD, Parton A, Groucutt HS, Alsharekh A (2015) Green Arabia: Human prehistory at the crossroads of continents. Quatern Int 382:1–7

Prescott JR, Stephan LG (1982) The contribution of cosmic radiation to the environmental dose for thermoluminescent dating. Latitude, altitude and depth dependencies. PACT 6:17–25

Prescott JR, Hutton JT (1988) Cosmic-ray and gamma-ray dosimetry for TL and electron-spin- resonance. Nuclear Tracks Radiation Measurements 14:223–227

Preston GW, Thomas DSG, Goudie AS, Atkinson OAC, Leng MJ, Hodson MJ, Walkington H, Charpentier V, Méry S, Borgi F, Parker AG (2015) A multi-proxy analysis of the Holocene humid phase from the United Arab Emirates and its implications for southeast Arabia's Neolithic populations. Quatern Int 382:277–292

Preusser F, Radies D, Matter A (2002) A 160,000-year record of dune development and atmospheric circulation in southern Arabia. Science 296:2018–2020

Preusser F (2009) Chronology of the impact of Quaternary climate change on continental environments in the Arabian Peninsula. Comptes Rendus Geosci 341:621–632

Rosenberg TM, Preusser F, Fleitmann D, Schwalb A, PenkmanK ST, Al-Shanti MA, Kadi K, Matter A (2011) Humid periods in southern Arabia: Windows of opportunity for modern human dispersal. Geology 39:1115–1118

Sakellariou D, Bailey GN, Momber G, Meredith-Williams M, Alsharekh A, Rousakis G, Panagiotopoulos I, Morfis I, Stavrakakis S, Pampidis I, Renieris P, Georgiou P, Kalogirou S, Mantopolos P, Stasinos V, Kallergis M, Manousakis L, Al Nomani SM, Devès M (2013) Preliminary report on underwater survey in the Farasan Islands by the R/V Aegaeo, May-June 2013. Technical Report, Hellenic Centre for Marine Research (HCMR), Athens, Greece

Sakellariou D, Rousakis G, Panagiotopoulos I, Morfis I, Bailey G (this volume) Geological structure and Late Quaternary

geomorphological evolution of the Farasan Islands continental shelf, south Red Sea, SW Saudi Arabia

Sanderson DCW (1988a) Fading of thermoluminescence of feldspars—characteristics and corrections. Nuclear Tracks Radiation Measurements 14:155–161

Sanderson DCW (1988b) Thick Source Beta-Counting (TSBC)—a rapid method for measuring beta-dose-rates. Nuclear Tracks Radiation Measurements 14:203–207

Sanderson DCW, Bishop P, Houston I, Boonsener M (2001) Luminescence characterisation of quartz-rich cover sands from NE Thailand. Quaternary Sci Rev 20:893–900

Sanderson DCW, Murphy S (2010) Using simple portable OSL measurements and laboratory characterization to help understand complex and heterogeneous sediment sequences for luminescence dating. Quat Geochronol 5:299–305

Scerri EML, Breeze PS, Parton A, Groucutt HS, White TS, Stimpson C, Clark-Balzan L, Jennings R, Alsharekh A, Petraglia MD (2015) Middle to Late Pleistocene human habitation in the western Nefud Desert, Saudi Arabia. Quatern Int 382:200–214

Scott EM, Sanderson DCW (1988) Statistics and the additive dose method in TL dating. Nuclear Tracks Radiation Measurements 14 (1/2):345–354

Sinclair A, Inglis RH, Shuttleworth, A, Foulds, FW, Alsharekh, AM (this volume) Landscape archaeology, Palaeolithic survey and coastal change along the southern Red Sea of Saudi Arabia

Singhvi AK, Sharma YP, Agrawal DP (1982) Thermoluminescence dating of sand dunes in Rajastan, India. Nature 295:313–315

Singhvi AK, Sharma YP, Agrawal DP, Dhir RP (1983) Thermoluminescence dating dune sands—some refinements. PACT 9(II):499–504

Stimpson CM, Breeze PS, Clark-Balzan L, Groucutt HS, Jennings R, Parton A, Scerri E, White TS, Petraglia MD (2015) Stratified Pleistocene vertebrates with a new record of a jaguar-sized pantherine (Panthera cf. gombaszogensis) from northern Saudi Arabia. Quatern Int 382:168–180

Thomsen KJ, Murray AS, Jain M, Bøtter-Jensen L (2008) Laboratory fading rates of various luminescence signals from feldspar-rich sediment extracts. Radiat Meas 43:1474–1486

Wang XL, Wintle AG, Lu YC (2006) Thermally transferred luminescence in fine grained quartz from Chinese loess, basic observations. Radiat Meas 41:649–658

Wallinga J, Murray A, Wintle A (2000) The single-aliquot regenerative-dose (SAR) protocol applied to coarse-grain feldspar. Radiation Measurements 32:529–533

Wilson JWP, Roberts GG, Hoggard MJ, White NJ (2014) Cenozoic epeirogeny of the Arabian Peninsula from drainage modeling. Geochem Geophys Geosyst 15:3723–3761

Winder IC, Deves MH, King GCP, Bailey GN, Inglis RH, Merridith-Williams M (2015) Evolution and dispersion of the genus *homo*: A landscape approach. J Human Evolution 87:48–65

Wintle AG, Huntley DJ (1979) Thermoluminescence dating of a deep-sea sediment core. Nature 279:710–712